Nucleic Acids Research, 2020 **1**
doi: 10.1093/nar/gkaa096

Site-specific proteolytic cleavage prevents ubiquitination and degradation of human REV3L, the catalytic subunit of DNA polymerase ζ

Fengting Wang†, Pan Li†, Yuan Shao, Yanyan Li, Kai Zhang, Miaomiao Li, Rong Wang, Shuo Zheng, Yingying Wang, Sen Song, Shiguo Feng, Fei Liu, Wei Xiao and Xialu Li*

Beijing Key Laboratory of DNA Damage Response and College of Life Sciences, Capital Normal University, Beijing, China

Received December 21, 2018; Revised February 02, 2020; Editorial Decision February 03, 2020; Accepted February 04, 2020

ABSTRACT

REV3L, the catalytic subunit of DNA polymerase ζ (Pol ζ), is indispensable for translesion DNA synthesis, which protects cells from deleterious DNA lesions resulting from various intrinsic and environmental sources. However, REV3L lacks a proofreading exonuclease activity and consequently bypasses DNA lesions at the expense of increased mutations, which poses a severe threat to genome stability. Here we report a site-specific proteolytic event of human REV3L. We show that REV3L is cleaved by a *th*reonine *asp*artase, Taspase1 (TASP1), to generate an N-terminal 70-kDa fragment (N70) and a polypeptide carrying the C-terminal polymerase catalytic domain in human cells. Strikingly, such a post-translational cleavage event plays a vital role in controlling REV3L stability by preventing ubiquitination and proteasome-mediated degradation of REV3L. Indicative of the biological importance of the above REV3L post-translational processing, cellular responses to UV and cisplatin-induced DNA lesions are markedly impaired in human HCT116 cell derivatives bearing defined point mutations in the endogenous *REV3L* gene that compromise REV3L cleavage. These findings establish a new paradigm in modulating the abundance of REV3L through site-specific proteolysis in human cells.

INTRODUCTION

DNA Polymerase ζ (Pol ζ) is the only B-family translesion DNA synthesis (TLS) polymerase, required for the bypass of a large variety of DNA lesions that impair replication fork progression (1,2). Unlike other high-fidelity B-family replicative polymerases, REV3, the catalytic subunit of Pol ζ, has no proofreading function due to the lack of an intrinsic 3′-5′ exonuclease activity (3). Consequently, REV3 shows relatively low fidelity and is responsible for the generation of the vast majority of spontaneous and DNA damage-induced mutations in eukaryotic cells (4–7).

The human homolog of REV3, encoded by the *REV3L* gene, contains 3130 residues, which is about twice the mass of its yeast counterpart (8). Of note, a spacer region between the highly-conserved N-terminal domain (1–333 a.a.) and the C-terminal polymerase domain (2276–3130 a.a.) has been massively expanded from ∼280 a.a. in yeast REV3 to ∼2000 a.a. in human REV3L (9). The functional relevance of this region in human REV3L remains largely elusive. Besides two adjacent binding motifs for REV7 (10–14), an accessary subunit of Pol ζ, and a positively charged domain that is conserved among vertebrate REV3 orthologs, the inserted sequences consist of mostly unstructured and low complexity segments without defined function (9). Intriguingly, while REV3 is dispensable for survival and proliferation in yeast (15), depletion of REV3L severely impairs normal cell proliferation, genome stability, and embryogenesis in mammals (16–24). A concerted evolution of both REV3 structure and function suggests a functional significance of the expanded sequences within the central domain of human REV3L, but this significance has not yet been determined.

Although REV3L is critical for cells to survive from deleterious DNA lesions resulting from various endogenous and environmental sources (8,9,23,25–30), its error-prone polymerase activity may pose a severe threat to genome integrity and needs to be tightly controlled. However, the mechanism by which the activity of REV3L is modulated remains enigmatic. Here, we describe an unexpected role of a site-specific proteolytic event in preventing ubiquitination and proteasome-mediated degradation of human REV3L and its significance for REV3L to function in response to UV and cisplatin-induced DNA lesions in human cells.

*To whom correspondence should be addressed. Tel: +86 10 68901441; Fax: +86 10 68902037; Email: 6239@cnu.edu.cn
†The authors wish it to be known that, in their opinion, the first two authors should be regarded as Joint First Authors.

These findings not only uncover a novel post-translational processing event of human REV3L, but more importantly, shed new light on the exquisite mechanisms by which the activity of an error-prone polymerase is modulated in human cells.

MATERIALS AND METHODS

Plasmids and reagents

To generate the targeting construct (#1) for integrating a 3xFLAG tag sequence immediately upstream to the start codon of the *REV3L* gene, a fragment consisting of sequences encoding a puromycin *N*-acetyl-transferase (Puro), a self-cleaving 2A peptide and a 3xFLAG tag in tandem, flanked by 1.6- and 2.0-kb genomic DNA fragments surrounding the start codon of the human *REV3L* gene, was cloned into the pBlueScript-KSII vector (Figure 1A). To generate the targeting construct (#2) for inserting a tetracycline (tet)-inducible promoter 5′ to *REV3L*, sequences between the two pieces of genomic DNA fragments in targeting construct #1 are replaced by a fragment carrying a *Hygromycin-B-phosphotransferase* (*hyg*) gene, a 3xpolyadenylation signal (3xPA), a tet-inducible promoter (P_{tet}) and the sequences encoding 3xFLAG tag (Supplementary Figure S9D and E). To generate the targeting construct (#3) for introducing defined mutations in exon thirteen of *REV3L,* a fragment consisting of two splice acceptor sites, the sequences encoding a 2A peptide, a Puro expression cassette and the sequences of a 3xPA signal, flanked by two *loxP* sites and ∼1.5-kb genomic DNA fragments surrounding the twelfth intron of the *REV3L* gene (Figure 5G, Supplementary Figure S9A–C), was cloned into the pL452 vector. Oligonucleotide pair #1 (F: CA CCGCTGCCGGG-TCGCCAGTGAA, R: AAACTTCA CTGGCGACCCGGCAGC) was cloned into pX330 (from Feng Zhang's lab, MIT) (31), generating pX330-REV3L-N for expression of both Cas9 and a guide RNA (gRNA) that targets Cas9 to a region immediately upstream to the start codon ATG of the *REV3L* gene. Oligonucleotide pairs #2 (F: CACCGTAACTGAGGTAT-AGAAAGAC, R: AAACGT CTTTCTATACCTCAGTTAC) and #3 (F: CACCGGAACT-GCAGATGAAAATAG, R: AAACCT ATTTTCATCTGCAGTTCC) were cloned into pX335-neo (modified from pX335 vector from Feng Zhang's lab, MIT) (31), generating pX335-neo-REV3L-D525A-Mut-1 and pX335-neo-REV3L-D525A-Mut-2 constructs, respectively, for expression of both the D10A mutant nickase version of Cas9 (Cas9n) and a pair of offset gRNAs complementary to opposite strands of the sequences encoding TASP1 cleavage site in the *REV3L* gene (Figure 5A). Oligonucleotide pair #4 (F: CACCGAAAAA-TGAGGT TTTCGCATT, R: AAACAATGCGAAAACCTCATTT TTC) and #5 (F: CACC-GATTTTGAGGCTAGGCGC T C, R: AAACGAGCGCCTAGCCTCAAAATC) were cloned into pX330, generating pX330-REV3L-D525A-Mut-1 and pX330-REV3L-D525A-Mut-2 constructs, respectively, for expression of both Cas9 and a pair of gRNAs that target Cas9 to two individual regions within the twelfth intron of the *REV3L* gene.

Human *TASP1* cDNA was cloned from HeLa cell cDNAs and inserted into the eukaryotic expression vector pcDNA3 (Invitrogen) and the N-terminal glutathione-S-transferase (GST)- and C-terminal 8xhistidine (His8) doubly-tagged bacterial expression vector pREST-GH. Human *REV3L* cDNAs were a generous gift from Dr C. Lawrence (University of Rochester Medical Center, Rochester, NY). Full-length and truncated *REV3L* cDNA variants were amplified by PCR and inserted into the modified pcDNA3 vectors that contain a Puro expression cassette and various tags as indicated in the text. PCR fragments, encoding REV3L a.a. 327–553 derived from either wild-type or different cleavage-deficient REV3L mutants, were inserted into a modified pREST-A vector containing sequences encoding an N-terminal GST tag. *TASP1* and *REV3L* mutants were generated by PCR-mediated site-directed mutagenesis. All the constructs were verified by DNA sequencing. Details of plasmid construction are available upon request.

Oligonucleotides and commercial antibodies used in this study are described in Supplementary Tables S1 and S2. A mouse monoclonal antibody against a REV3L fragment (residues 327–553) was developed in the lab. The specificity of the lab-made REV3L antibody was verified in REV3L-depleted cells (Supplementary Figure S4A). Glycerol stocks of shRNAs were obtained from the Sigma Mission library. All other reagents were Sigma-Aldrich products unless noted.

Cell culture, transfection and lentivirus-based transduction

Human embryonic kidney (HEK) cell line 293 (Life Technologies) and HeLa cells (ATCC) were maintained in Dulbecco's modified Eagle's medium (DMEM) supplemented with 10% fetal bovine serum (FBS, PAN Biotech, Germany) and 2 mM GlutaMAX (Life Technologies) at 37°C with 5% CO_2. HCT116 cells (ATCC) were maintained in Iscove's modified Dulbecco's medium (IMDM) supplemented with 10% FBS and 2 mM GlutaMAX at 37°C with 5% CO_2. Cell lines used in this study are described in Supplementary Table S3.

For transient transfection in HEK293 cells, cells were transfected using a calcium phosphate method and harvested for subsequent functional analyses 36 h after transfection. For stable transfection, linearized expression constructs were transfected into cells using Lipofectamine 3000 reagent following the manufacturer's instructions (Life Technologies). Stable transfectants were selected in medium containing 800 μg/ml G418 or 300 ng/ml puromycin (Life Technologies) for 2 weeks. Transfection of siRNAs into HeLa cells by Lipofectamine 2000 was conducted following the manufacturer's instructions (Life Technologies).

Lentiviruses were prepared following the Lentiweb Protocol (https://www.addgene.org/protocols/lentivirus-production/). Virus was collected 48 h after transfection, filtered through a 0.4-μm membrane, and used directly to infect cells in the presence of 8 μg/ml polybrene.

CRISPR/Cas9-mediated targeting in HCT116 cells

To generate the endogenously N-terminal-tagged 3xFLAG-REV3L lines in HCT116 cells, the targeting construct #1 and the pX330-REV3L-N plasmid were transfected

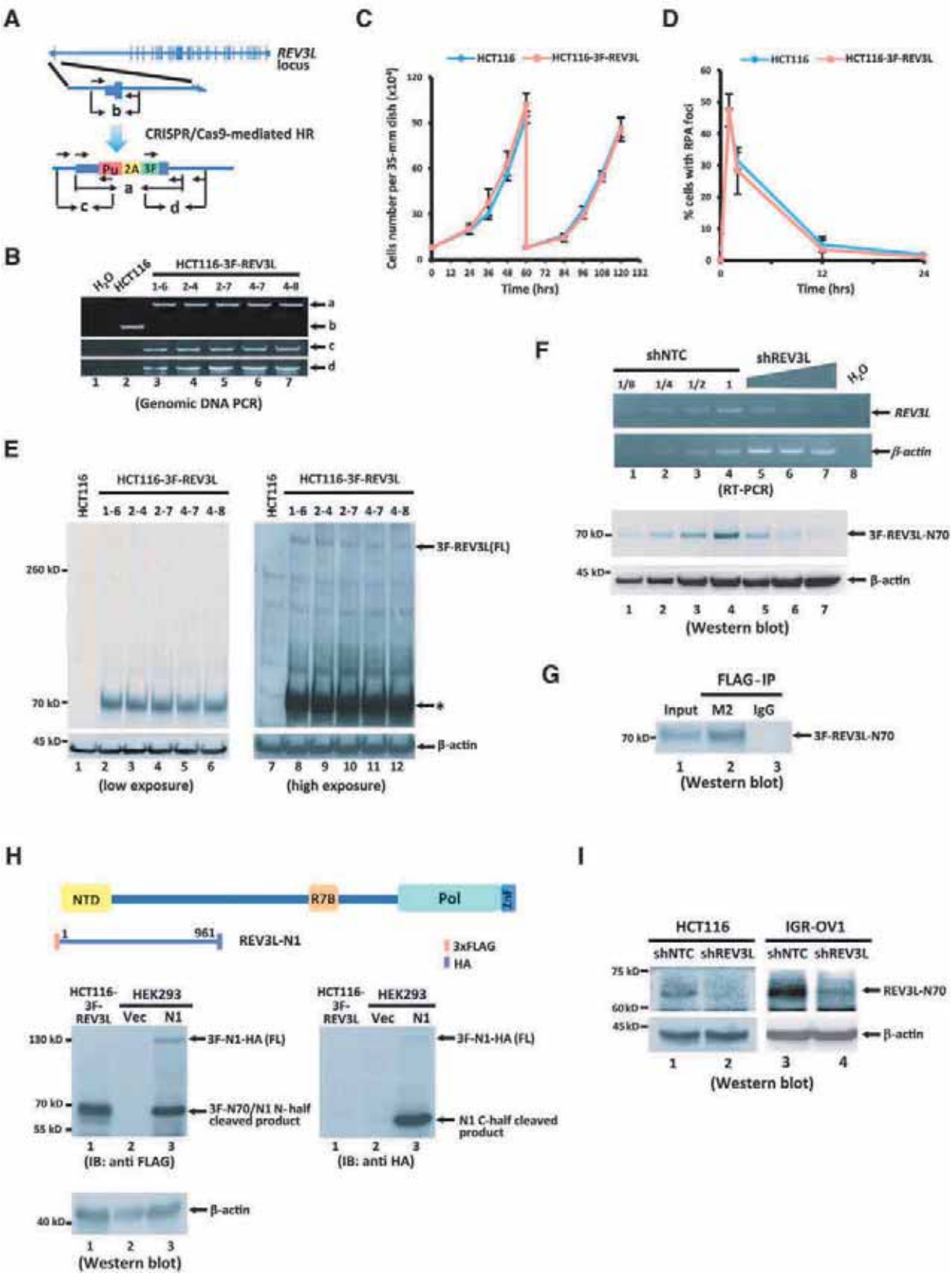

Figure 1. Human REV3L is proteolytically cleaved in a sequence-dependent manner. (**A**) Schematic of gene targeting strategy. A puromycin-selection cassette (Pu), a 2A peptide (2A) and a 3xFLAG tag (3F) are indicated. (**B**) Genotyping by genomic DNA PCR. Locations of PCR primers are indicated

together into HCT116 cells using Lipofectamine 3000 reagent. The cells were selected in medium containing 300 ng/ml puromycin for 12 days. Clones were screened by genomic DNA PCR using primers flanking the gRNA targeted region and by western blot for FLAG-tagged REV3L on whole cell lysates. The precise integration of the 3xFLAG-encoding sequences to the 5′-end of the coding region of the *REV3L* gene was further verified by directly sequencing the PCR fragments amplified from genomic DNA.

To generate *REV3L* conditional knockout HCT116-R-3F-REV3L cells, the targeting construct #2 and the pX330-REV3L-N plasmid were transfected together into HCT116 cells essentially as described above. The cells were selected in medium containing 300 μg/ml hygromycin B for 12 days. Positive clones, both homozygously and heterozygously targeted, were selected as described in the text.

To generate cleavage-deficient HCT116-3F-REV3L-TD-mut cells, the single-stranded donor oligonucleotides (ssODN), and the pX335-neo-REV3L-Mut-1 and -Mut-2 plasmids were transfected into HCT116 cells together as described above. Cells were subsequently selected in medium with 800 μg/ml G418 for 3 days and then continuously grown in regular medium for ten more days. Clones were screened for incorporation of the defined mutations at both alleles by BanI restriction enzyme digestion of the PCR fragments amplified from genomic DNA. Successful sequence conversion was further verified by sequencing the corresponding PCR products directly.

The HCT116-3F-REV3L-D525A-Mut(het) cell line was generated by two steps (Figure 5G). First, the 3′ half of the twelfth intron and the thirteenth exon of the *REV3L* gene in the heterozygous HCT116-3F-REV3L cells was substituted with a fragment containing a splice acceptor site and a Puro expression cassette, flanked by two *loxP* sites, a second splice acceptor site and a mutated exon thirteen of the *REV3L* gene bearing defined point mutations via CRISPR/Cas9-mediated homologous recombination as described above. The Puro expression cassette in the positive colony was subsequently excised by transient expression of Cre recombinase. Precise splicing of the RNA transcribed from the mutant *REV3L* allele was verified by directly sequencing the RT-PCR fragments.

HCT116-R-3F-REV3L-CI-mut(het) cells were generated by sequentially inserting defined mutations into the thirteenth exon of one *REV3L* gene and then a tet-inducible promoter 5′ for the second *REV3L* gene in HCT116 cells (Figure 8A). Transfection and screening were performed essentially as described above for generating HCT116-R-3F-REV3L and HCT116-3F-REV3L-D525A-mut(het) cells, respectively.

DNA, RNA, protein analyses

Genomic DNA and total RNA purification, PCR, RT-PCR and western blot were performed as described (32).

Recombinant protein expression and purification

GST, GST-tagged REV3L-N5 derivatives (WT/D525A/G526A/TD527,529AA) and GST-His doubly-tagged TASP1 proteins (WT and mutant) were expressed in *Escherichia coli* grown at 18°C in the presence of 0.1 mM IPTG. Sixteen hours after induction, bacteria were collected, washed with ice-cold PBS, and then suspended in lysis buffer containing 50 mM Tris–HCl (pH 7.9), 100 mM NaCl, 10% glycerol, 0.5% NP40, 1 mM DTT and 0.5 mM PMSF. Cells were disrupted by sonication at 20% continuous setting for 5 s 40 times with a 10 s incubation on ice between bursts, and the lysates were centrifuged at 16 500 × *g* for 20 min at 4°C.

For purification of GST and GST-tagged REV3L-N5 derivatives, the supernatant was loaded onto a glutathione Sepharose 4B column and eluted with buffer containing 50 mM Tris–HCl (pH 8.0), 150 mM NaCl, 0.2% NP40 and 20 mM reduced glutathione. The eluted proteins were dialyzed against buffer containing 50 mM Tris–HCl (pH 7.9), 100 mM NaCl, 0.2 mM EDTA, 0.5 mM DTT and 20% glycerol. Protein aliquots were stored at −80°C.

A tandem two-step affinity purification was applied to purify the GST-His8 doubly-tagged proenzyme of TASP1 and its mutant. For this, the cell lysates were first loaded on the glutathione Sepharose 4B column as described above. After washing the GST-resins with lysis buffer and PreScission Protease cleavage buffer [50 mM Tris–HCl (pH 7.9), 150 mM NaCl, 5 mM β-mercaptoethanol, 0.5 mM PMSF, 0.5% NP40], on-column PreScission Protease cleavage was performed overnight at 4°C. The flow-through was collected and loaded on a Ni-NTA resin column (Qiagen) in the presence of 50 mM Tris–HCl (pH 7.9), 150 mM NaCl, 0.5% NP40, 15 mM imidazole and 5 mM β-mercaptoethanol. The captured proteins were eluted with

←

in (A). (**C**) Growth curve of HCT116 and its derivative HCT116-3F-REV3L (clone #4–8) cells. (**D**) Time course of accumulation and clearance of UV-induced RPA foci. For each cell line at each time point at least 100 cells were counted. Error bars in (C) and (D) represent standard deviations from three independent experiments. Diamond, HCT116 cells. Square, HCT116-3F-REV3L cells. **(E)** Expression of 3xFLAG-tagged REV3L and β-actin was monitored by western blot in HCT116 cells and the genotyping-positive HCT116-3F-REV3L colonies. A band migrating at 70-kDa is indicated by an asterisk. (**F**) Depletion of REV3L in the positively-targeted cells by shRNA virion transduction. Seventy-two hours after infection, cells were assayed for the indicated mRNAs and proteins by RT-PCR (top panel) and western blot (bottom panel), respectively. Serial dilutions of the total RNAs and the whole cell lysate from the control shRNA (shNTC)-infected cells were used to quantify depletion efficiency of the *REV3L* mRNAs and proteins, respectively. Dilution factors are indicated. (**G**) Immunoprecipitation of the 70-kDa fragment by anti-FLAG antibody-conjugated M2 agarose. Anti-mouse IgG-coated agarose was used as the control. The eluted proteins were analyzed by western blot using an antibody against FLAG tag. (**H**) C-terminal-truncated REV3L-N1 is proteolytically cleaved in transient-transfection assays. Top panel: Schematic of the 3xFLAG and HA doubly-tagged REV3L-N1 truncation. Whole cell lysates were assayed for 3xFLAG-tagged (IB: anti FLAG) and HA-tagged (IB: anti HA) REV3L-N1 proteins by western blot. β-actin was detected as a loading control. Vec, vector. N1, REV3L-N1. Orange box represents a 3xFLAG tag. Purple box represents an HA tag. (**I**) The N-terminal cleavage product of endogenous REV3L exists in human cells. HCT116 and IGR-OV1 cells were transduced by either control (shNTC) or REV3L (shREV3L) shRNAs for 3 days. REV3L-N70 was monitored by western blot using an antibody against the N-terminus of the endogenous REV3L protein (top panel). β-actin was detected as a loading control (bottom panel).

buffer containing 20 mM Tris–HCl (pH 7.9), 500 mM NaCl, 10% glycerol, 500 mM imidazole and 1 mM DTT. The eluted proteins were dialyzed against buffer containing 50 mM Tris–HCl (pH 7.9), 20 mM KCl, 0.2 mM EDTA, 5 mM DTT and 20% glycerol. Protein aliquots were stored at −80°C.

TASP1 *in vitro* cleavage assay

An *in vitro* cleavage assay was performed essentially as described (33). 1.8 μg recombinant protein (GST or GST-REV3L-N5 derivatives) was incubated with the indicated amount of purified WT or mutant TASP1 protein in a volume of 20 μl of reaction [100 mM HEPES (pH 7.9), 5 mM $MgCl_2$, 20 mM KCl, 5% glycerol, 5 mM DTT] at 37°C for various times as indicated in the text. Reactions were stopped by rapidly mixing with 6.5 μl of 4× loading buffer [200 mM Tris–HCl (pH6.8), 8% SDS, 0.2% bromophenol blue, 40% glycerol] and incubating at 70°C for 10 min. The heat-inactivated reactions were resolved on a 10% SDS-PAGE gel and analyzed by colloidal blue staining or Coomassie blue staining.

UV-induced RPA nuclear focus assay

Cells were seeded on coverslips coated with 0.01% poly-L-lysine 24 h before UV irradiation. The culture medium was removed and cells in a 35-mm dish were exposed to 254-nm UV irradiation from a low-pressure mercury lamp (G8T5, Sankyo Denki). The dose rate was measured using a UVX Radiometer (UVP) equipped with a 254-nm detector. Samples for comparison in each panel were treated identically. RPA nuclear foci were detected as described (34). A Ni-E (Nikon) microscope connected to a Zyla sCMOS (VDG-152V-C1E-FI) digital camera (Andor) and run by NIS-Elements AR software (Nikon) was used for image acquisition.

Immunoprecipitation and denaturing His-ubiquitin pull down

For denaturing anti-FLAG immunoprecipitation, cell pellets were suspended into one packed cell volume (PCV) of 8 M urea lysis buffer [8 M urea, 100 mM Tris–HCl (pH 7.5), 1% Triton X-100]. The cell suspension was forced through a 21 gauge needle 10 times and subsequently rotated at room temperature for 30 min. The lysate was subjected to nuclease digestion by adding two PCV of nuclease digestion buffer [50 mM Tris–HCl pH7.5, 0.02% Triton X-100, 4 mM $MgCl_2$] with 100 U/ml benzonase (Sigma). After a 30-min incubation at room temperature, the lysate was mixed with four PCV of dilution buffer [50 mM Tris–HCl, 1% Triton X-100, 360 mM NaCl] and incubated with anti-FLAG antibody-conjugated M2-agarose beads (Sigma) overnight at 4°C. Immunoprecipitants were washed five times with wash buffer [50 mM Tris–HCl pH 7.5, 1 M urea, 500 mM NaCl, 0.1% NP40, 0.2 mM EDTA] before being resolved by SDS-PAGE and immunoblotted with indicated antibodies.

For identification of immunoprecipitants by mass spectrometry (MS) analyses, the immunopurified polypeptides were eluted with the 0.2 mg/ml 3xFLAG peptide in elution buffer [50 mM Tris–HCl (pH 7.5), 150 mM NaCl, 0.5% Triton X-100, 0.2 mM EDTA] and resolved on a 4–20% gradient SDS-PAGE gel for colloidal blue staining analysis. A band at 70 kDa was cut out from the gel and subjected to MS analysis. Protein identifications by LC-MS/MS were performed at Beijing Protein Innovation and at the Proteomics Facility of the National Institute of Biological Sciences (NIBS), Beijing.

For co-immunoprecipitation (Co-IP) of endogenous 3xFLAG-REV3L-associated nuclear proteins, nuclei of HCT116-3F-REV3L cells were prepared as described (35). The isolated nuclei were suspended into RIPA buffer [45 mM HEPES (pH 7.9), 450 mM NaCl, 1% Triton X-100, 1 mM DTT, protease inhibitor cocktail (Sigma)] and subjected to sonication at 15% continuous setting for 5 s three times with a 30-s incubation on ice between bursts. The lysate was diluted by adding three volumes of buffer containing [45 mM HEPES (pH 7.9), 1 mM DTT, protease inhibitor cocktail (Sigma), 2 mM MgCl, 1 mM $CaCl_2$, 100 U/ml Benzonase, 50 μg/ml RNaseA]. After incubation at 4°C for 30 min, the lysate was centrifuged at 16 500 × *g* for 10 min at 4°C. The supernatant was collected and mixed with washed anti-FLAG antibody-conjugated M2-agarose beads (Sigma) overnight at 4°C. Captured proteins were eluted with buffer containing 20 mM HEPES (pH 7.9), 500 mM NaCl, 1% Triton X-100, 0.2 mM EDTA and 0.2 mg/ml 3xFLAG peptide and subjected to MS analysis.

For reciprocal Co-IP of tagged-REV3L truncations transiently expressed in HEK293 cells, cells were harvested 48 h after transfection. The whole cell extract was prepared and subjected to anti-FLAG or anti-HA immunoprecipitation essentially as described above.

For the denaturing His-ubiquitin pull-down assay, cells were transfected with plasmids expressing His8-tagged ubiquitin or ubiquitin mutants. Twenty-four hours post-transfection, cells were treated with MG132 (10 μM for 10 h) and then subjected to the purification of His8-tagged proteins by Ni-NTA beads (Qiagen). The cell pellet was lysed in buffer containing 6 M guanidine hydrochloride, 0.1 M Tris–Cl (pH 7.4), and the lysate was then incubated with Ni-NTA beads for 3 hrs at room temperature. The beads were washed with buffer containing 8 M urea, 100 mM Tris–HCl (pH 7.4), 1% NP40, 1 M NaCl and 20 mM imidazole, and the ubiquitin-conjugated proteins were analyzed by immunoblot.

SupF mutagenesis assay

The *supF* shuttle vector-based mutagenesis assay was performed essentially as described (36). Briefly, the corresponding HCT116 derivatives were transfected with mock-treated or UV-C-irradiated pSP189 shuttle plasmids. Two days after transfection, the plasmids were retrieved using a DNA miniprep kit (Tiangen, China). The purified plasmids were digested with *Dpn*I (NEB, 4 h, 37°C) and subsequently transformed into MBM7070 *E. coli*. Transformants were selected on LB plates containing 10 mM IPTG, 20 mg/ml X-gal and 80 μg/ml ampicillin. The mutation frequency was calculated as the ratio of white colonies (mutant) to total colonies.

RESULTS

A proteolytic event of human REV3L

To facilitate identification of REV3L and rapid purification of REV3L-associated proteins, we established a human HCT116 cell derivative, named HCT116-3F-REV3L, in which the 3xFLAG tag coding sequence was inserted 5′ to *REV3L* in-frame by CRISPR/Cas9-mediated chromosomal integration (Figure 1A). Colonies that had undergone homologous recombination on both alleles of the *REV3L* gene were identified by genomic DNA PCR (Figure 1B). The precise integration of the 3xFLAG tag sequence immediately upstream to the *REV3L* coding region was confirmed by sequencing the corresponding region in the genome (Supplementary Figure S1A and B).The inserted exogenous sequences slightly increase the steady levels of the *REV3L* mRNA (∼50%) in HCT116-3F-REV3L cells in comparison with those in its parental HCT116 cells (Supplementary Figure S1C).

Depletion of REV3L significantly impairs cell growth in HCT116 cells (Supplementary Figure S2, Figure 1F, top panel). Indicative of a competent function of 3F-REV3L, the growth rate of HCT116-3F-REV3L cells is comparable to that of parental HCT116 cells (Figure 1C). Importantly, the kinetics of formation and clearance of UV-induced replication protein A (RPA) foci, an indicator for single-stranded DNA (ssDNA) regions at the stalled replication forks (37), in HCT116-3F-REV3L cells is indistinguishable from those of parental HCT116 cells (Figure 1D). REV3L is an indispensable TLS DNA polymerase involved in bypassing UV-induced DNA lesions in human cells (26) (Supplementary Figure S10A and S10B). Since 3F-REV3L is the only expressed REV3L protein in HCT116-3F-REV3L cells, we conclude that 3F-REV3L fully complements the function of REV3L required for cell growth and cellular response to UV damage in HCT116 cells.

Consistent with a precise fusion of a 3xFLAG tag to the N-terminus of REV3L, an antibody against the FLAG tag detects a protein appropriate for the full-length 3F-REV3L (migrates at ∼350-kDa) from the lysates of HCT116-3F-REV3L cells, but not from those of parental HCT116 cells (Figure 1E, right panel). Remarkably, the anti-FLAG antibody simultaneously recognizes a ∼70-kDa fragment in much larger quantities than the full-length REV3L in the lysates of HCT116-3F-REV3L cells (Figure 1E). Several lines of evidence indicate that the 70-kDa fragment is a truncation product of 3F-REV3L. First, in contrast to the cells expressing the control shRNA (shNTC), the amount of the 70-kDa fragment is markedly decreased in HCT116-3F-REV3L cells expressing the shRNA specifically targeting the *REV3L* gene in a dose-dependent manner (Figure 1F, bottom panel, lanes 5–7 in comparison with lane 4). Second, the 70-kDa fragment is specifically immunoprecipitated by an anti-FLAG antibody under a denaturing condition (in the presence of 1 M urea), whereas no signal is detected when mouse IgG is used for immunoprecipitation in parallel (Figure 1G). Third, by employing MS analysis, we identified 45 tryptic fragments from the immunoprecipitated 70-kDa fragment, which map to a region from residues 34 to 398 in REV3L (Supplementary Figure S3). This 70-kDa fragment is referred to as N70 in the subsequent experiments.

Of note, while the steady-state levels of N70 are much more abundant than those of the 350-kDa full-length REV3L in HCT116-3F-REV3L cells, we failed to detect any alternative mRNA isoform that might encode N70. Consistently, no relative mRNA isoform could be deduced from two published HCT116-derived poly(A)+ RNA sequencing (RNA-seq) libraries (The ENCODE Project Consortium 2012, ENCSR000CWM). These facts raised the possibility that N70 is a product resulting from post-translational cleavage. To test this hypothesis, an N-terminal 3xFLAG and C-terminal HA doubly-tagged reporter, which contains the sequences encoding the extreme N-terminal 961 residues of REV3L (theoretical molecular mass, 107.8-kDa, referred to as REV3L-N1, Figure 1H), was transiently expressed in HEK293 cells. A 130-kDa fragment, appropriate for the full-length REV3L-N1, is detected by both anti-FLAG and anti-HA antibodies in the transfected HEK293 cells (Figure 1H, middle left panel, lane 3). Strikingly, we simultaneously detected a ∼70-kDa FLAG-tagged fragment and a ∼58-kDa HA-tagged fragment in the reporter-transfected cells (Figure 1H, lane 3 in middle left and right panels), indicating the existence of a proteolytic event of REV3L-N1 in these cells. More importantly, by taking advantage of a monoclonal antibody specifically recognizing N70 (Supplementary Figure S4A), we detected a ∼70-kDa fragment in the lysates from two human cell lines and several mouse tissues (Figure 1I and Supplementary Figure S4B). Significantly, levels of the 70-kDa protein were markedly reduced upon transduction of shREV3L virion in both HCT116 and IGR-OV1 cell lines (Figure 1I). Together, our data support that REV3L undergoes a previously-unrecognized proteolytic event in human cells.

REV3L is proteolytically cleaved in a sequence-dependent manner *in vivo*

To localize the cleavage site, a series of REV3L N-terminal reporters were generated and transiently transfected into HEK293 cells (Figure 2A, left panel). The integrity of the relative REV3L truncations was analyzed by western blot using antibodies against the N-terminal 3xFLAG tag and the C-terminal HA tag. Analogous to the REV3L-N1 reporter, both a full-length REV3L truncation and a ∼70-kDa fragment are detected by an anti-FLAG antibody in cells transfected with REV3L-N2 (encoding N-terminal 553 a.a. of REV3L) or -N3 (encoding N-terminal 541 a.a. of REV3L) reporter (Figure 2A, right panel, lanes 4 and 5). In contrast, only a single fragment migrating slightly slower than N70 is detected by both antibodies in REV3L-N4 reporter (encoding N-terminal 520 a.a. of REV3L) transfected cells (Figure 2A, right panel, lane 6). These data suggest that the proteolytic cleavage site(s) of REV3L resides between residues 520 and 541.

We next wished to precisely determine the amino acid requirement for REV3L cleavage in transient-transfection assays by utilizing sequential 7-aa substitutions followed by

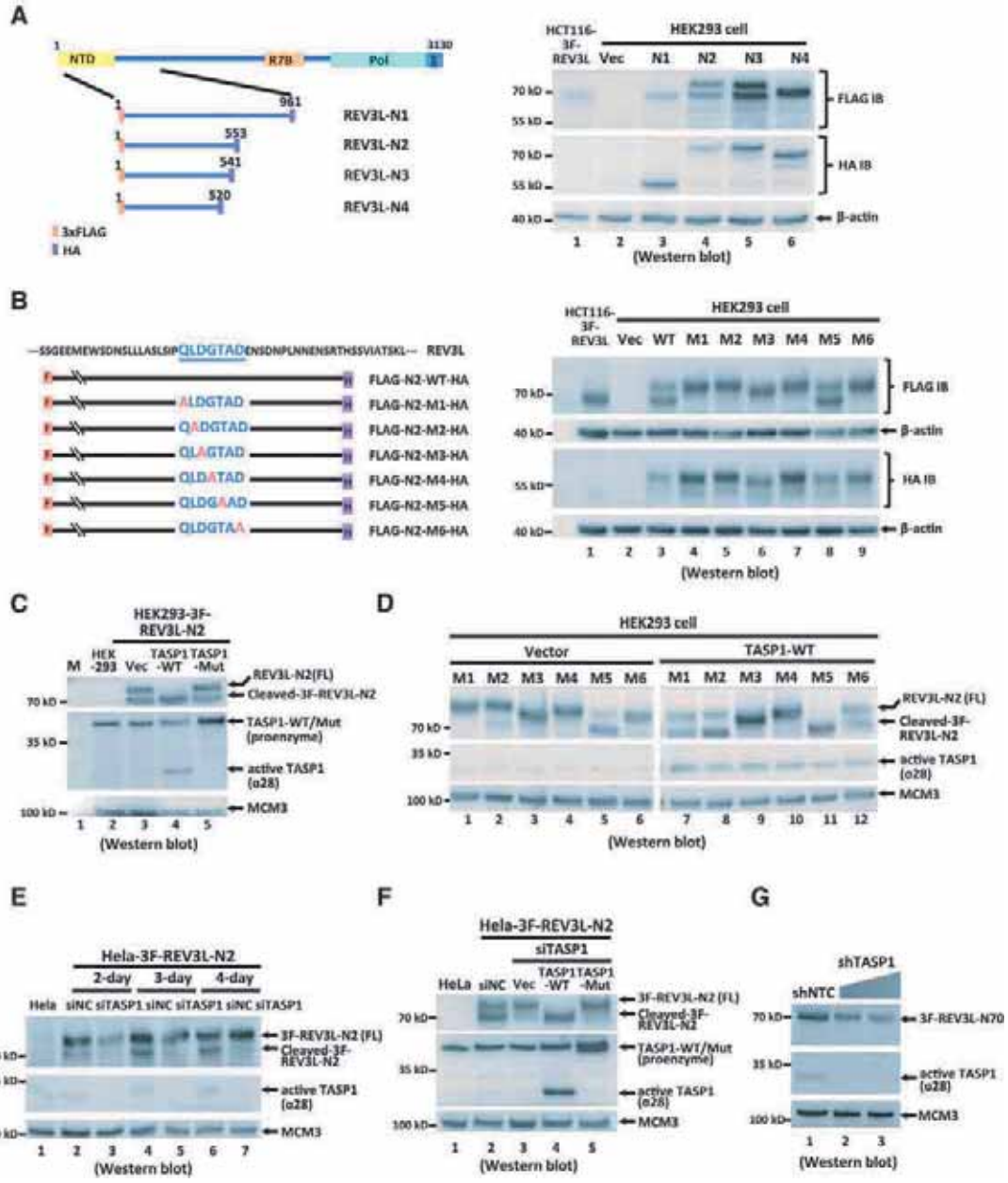

Figure 2. TASP1 cleaves human REV3L *in vivo*. (**A**) REV3L is proteolytically cleaved between a.a. 520–541. Left panel: Schematic of the 3xFLAG and HA doubly-tagged REV3L truncations that were transiently expressed in HEK293 cells. Orange box represents a 3xFLAG tag. Purple box represents an HA tag. Right panels: Whole cell lysates were assayed for 3xFLAG-tagged and HA-tagged REV3L truncations by western blot. β-actin was detected as a loading control. Vec, vector. (**B**) Determination of essential amino acids for the proteolytic cleavage of REV3L. Left panel: Schematic of alanine substitutions in the REV3L-N2 truncation. Cleavage-critical residues are highlighted in blue, whereas the alanine substitution is in red. Right panel: Whole cell lysates were subjected to western blot analysis as described in (A). (**C**) Overexpression of TASP1 facilitates cleavage of REV3L-N2 truncation in transient-transfection assays. The 3F-REV3L-N2 expression construct was transfected together with vector (Vec), wild-type (TASP1-WT) or mutant (TASP1-Mut) TASP1 expression constructs in HEK293 cells. Forty eight hours after transfection, cleavage products (top panel) and TASP1 (middle panel) were monitored by western blot. Mock-transfected HEK293 cells were used as a negative control for anti-FLAG immunoblotting. MCM3 was detected as a loading control. (**D**) D525 and G526 are essential for the cleavage of REV3L-N2 by TASP1 *in vivo*. 3F-REV3L-N2 mutants were transfected together with either vector or wild-type TASP1 (TASP1-WT) in HEK293 cells, and cleavage products were analyzed as described in (C). (**E**) Depletion of endogenous TASP1 suppresses cleavage of REV3L-N2 in HeLa cells. HeLa-3F-REV3L-N2 cells, stably expressing 3F-REV3L-N2 truncation, were treated with either control (siNC) or TASP1 siRNA (siTASP1) for 2, 3 or 4 days. Cleavage products (top panel), active TASP1 α28 (middle panel) and MCM3 (bottom panel) were monitored as described in (C). HeLa cells were used as the negative control for anti-FLAG immunoblotting. (**F**) Exogenous TASP1 rescues cleavage of REV3L-N2 in TASP1 siRNA-treated HeLa cells. TASP1 siRNA were transfected together with vector, wild-type or mutant TASP1 expression constructs in HeLa-3F-REV3L-N2 cells for 3 days. Cleavage products (top panel), TASP1 (middle panel) and MCM3 (bottom panel) were examined as described in (C). (**G**) Depletion of TASP1 suppresses cleavage of endogenous REV3L in HCT116-3F-REV3L cells. Cleavage of endogenous 3F-REV3L was examined in cells transduced by either control (shNTC) or TASP1 (shTASP1) shRNAs for 4 days. N70 (top panel), active TASP1 α28 (middle panel) and MCM3 (bottom panel) were monitored as described in (C).

alanine scanning mutagenesis, covering residues from 521 to 540 in the REV3L-N2 reporter. Our data show that a single alanine substitution at residue Q523, L524, D525, G526 or D529 markedly blocks the cleavage of REV3L-N2 (Figure 2B, right panel, lanes 4–7 and lane 9), indicating that the Q-L-D-G-T-A-D motif is critical for the proteolytic cleavage of REV3L-N2 truncation *in vivo*.

TASP1 is the protease responsible for the proteolysis of human REV3L at the Q-L-D-G-T-A-D motif

Notably, the Q-L-D-G-T-A-D motif virtually contains a known cleavage site (QLD/G) of TASP1, a *t*hreonine *asp*artase (33,38,39). We thus asked whether TASP1 is the protease responsible for REV3L cleavage at the Q-L-D-G-T-A-D motif. In agreement with this hypothesis, the cleavage of REV3L-N2 is sharply increased in HEK293 cells overexpressing the wild-type human TASP1, but not the TASP1-T234A mutant deficient in autoproteolysis of the TASP1 proenzyme into the active α-β heterodimer (33) (Figure 2C). TASP1 overexpression also significantly enhances the cleavage of Q523A, L524A, T527A and D529A mutants to various degrees (Figure 2D, lanes 7, 8, 11 and 12 in comparison with lanes 1, 2, 5 and 6), whereas neither D525A nor G526A mutant is cleaved even in the presence of excessive TASP1 (Figure 2D, lanes 9 and 10 in comparison with lanes 3 and 4). These data indicate that residues D525 and G526 are absolutely required for the cleavage of REV3L-N2 by TASP1, in agreement with reports that TASP1 specifically cleaves its substrate after an aspartate residue and both aspartate and the following glycine are essential for TASP1-mediated cleavage at the QLD/G motif of MLL (33,39,40).

To ask whether endogenous TASP1 is capable for REV3L-N2 cleavage, we utilized an RNA interference approach to deplete TASP1 in HeLa cells stably expressing REV3L-N2. Cells were transfected with either TASP1 (siTASP1) or control (siNC) siRNA duplex and analyzed for TASP1 protein levels as well as the cleavage of REV3L-N2 at different time points following transfection. Concomitant with the depletion of TASP1 (Figure 2E, middle panel, lanes 3, 5 and 7), cells transfected with the siTASP1 but not the siNC exhibit a marked decrease in the protein levels of the cleaved REV3L-N2 (Figure 2E, top panel, lanes 3, 5, 7 in comparison with lanes 2, 4, 6). Importantly, overexpression of exogenous TASP1 not only rescues but significantly enhances the cleavage of REV3L-N2 in the siTASP1-transfected HeLa-3F-REV3L-N2 cells (Figure 2F, lane 4 in comparison with lanes 2 and 3). In contrast, overexpression of the TASP1-T234A mutant has no discernible effects on the cleavage of REV3L-N2 in these cells (Figure 2F, lane 5 in comparison with lane 3).

To assess whether TASP1 is indeed responsible for the cleavage of endogenous REV3L in human cells, we introduced either a TASP1 (shTASP1) or control (shNTC) shRNA expression cassette into HCT116-3F-REV3L cells by lentiviral transduction. Stable expression of shTASP1, but not the control shNTC, sharply decreases the protein level of the active TASP1 α28 in HCT116-3F-REV3L cells (Figure 2G, middle panel, lanes 2 and 3 in comparison with lane 1). Concomitantly, the cleavage of the endogenous 3F-REV3L is markedly impaired upon TASP1 depletion, reflected in a significant decrease in the steady-state levels of the N-terminal cleavage product N70 in the shTASP1-virion transduced cells in comparison with those in the shNTC-virion transduced cells (Figure 2G).

To obtain direct evidence that REV3L is a substrate of TASP1, we set out to establish an *in vitro* cleavage assay by using recombinant human TASP1 proteins, both wild-type and the T234A mutant, and an N-terminal GST-tagged REV3L truncation N5 (residues 327–553) carrying the Q-L-D-G-T-A-D motif essential for REV3L proteolytic cleavage *in vivo* (Figure 3A). Consistent with the necessary and sufficient role of TASP1 on REV3L cleavage *in vivo*, the recombinant wild-type TASP1 directly proteolyzes REV3L-N5 in a dose-dependent manner *in vitro* (Figure 3B, lanes 2–6). The cleavage of REV3L-N5 by TASP1 is specific because the recombinant TASP1-T234A mutant, even presented at a high protein concentration and for an extended incubation time, is unable to cleave REV3L-N5 *in vitro* (Figure 3B, lanes 7–11; Figure 3C, bottom panel). We also found that, analogous to what was observed in the aforementioned transient-transfection assays, amino acid substitution of either D525 or G526 with alanine on REV3L-N5 completely abolishes its cleavage by TASP1 *in vitro* (Figure 3D, middle two panels). In contrast, the N5-TD527,529AA mutant is cleaved in the presence of excessive TASP1 (Figure 3D, bottom panel). These data, together with the above *in vivo* studies, unequivocally show that TASP1 is the primary protease for the cleavage of REV3L within the Q-L-D-G-T-A-D motif.

Cleavage products form a post-cleavage complex in human cells

Intriguingly, by employing MS analysis, we detected 30 tryptic peptides that match the sequences of REV3L from the polypeptides immunoprecipitated by an anti-FLAG antibody from the nuclear extract of HCT116-3F-REV3L cells (Figure 4A and B). Among them, 8 peptides map to a region within N70 (between residues 85 and 398, referred to as Region-1), whereas the remaining 22 peptides map to a region overlapping with the main part of the polymerase catalytic domain of REV3L within the C-terminus of REV3L (residues 2211–3073, referred to as Region-2). As a control, none of the REV3L-relative peptides are detected by MS in the polypeptides enriched by the anti-FLAG antibody from the nuclear extract of HCT116 cells (data not shown).

Because steady-state levels of the full-length REV3L are at least two orders of magnitude less than those of its N-terminal cleavage product N70 in the nuclear extract of HCT116-3F-REV3L cells (Supplementary Figure S5), we infer that the MS-detected peptides mapped to the Region-2 of REV3L are not derived from the trace amount of the full-length REV3L that might exist in the nuclear extract of HCT116-3F-REV3L cells. Instead, peptides from Region-2 are most likely derived from the C-terminal proteolytic products of REV3L co-purified with the 3xFLAG-tagged N70 from the nuclear extract. These results thus raise a possibility that after cleavage, N70 remains associated with the C-terminal cleavage product that carries a conserved

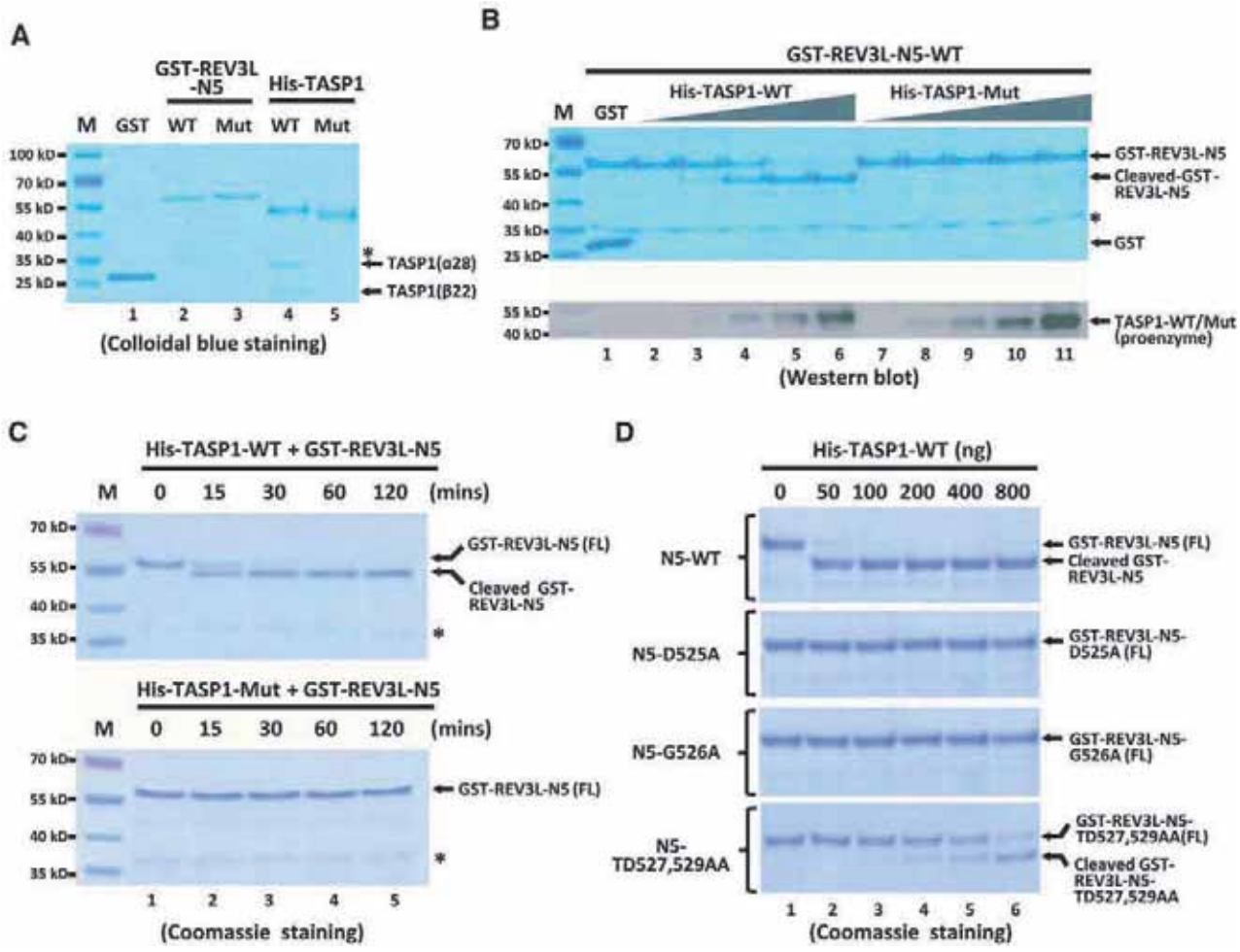

Figure 3. TASP1 directly cleaves human REV3L-N5 truncation *in vitro*. (**A**) Colloidal blue staining of recombinant proteins purified from *E. coli*. An unknown protein copurified with REV3L-N5 is indicated by an asterisk. The autoproteolyzed TASP1 fragments are indicated. (**B**) Dose-dependent cleavage of REV3L-N5 by TASP1 *in vitro*. 1.8 μg of GST-REV3L-N5 was incubated with 0, 50, 100, 200 or 400 ng of the wild-type TASP1 (TASP1-WT) or the TASP1-T234A mutant (TASP1-Mut) at 37°C for 30 mins. Samples were then resolved by 10% SDS-PAGE. All proteins used are recombinant proteins purified from *E. coli*. The amount of TASP1 in each reaction was monitored by western blot using an anti-TASP1 antibody (bottom panel). (**C**) Time course of TASP1-mediated cleavage of REV3L-N5 *in vitro*. 1.8 μg of GST-REV3L-N5 was incubated with 400 ng TASP1-WT or TASP1-Mut at 37°C for the indicated times. (**D**) D525 and G526 are essential for the cleavage of REV3L-N5 by TASP1 *in vitro*. The indicated amounts of TASP1-WT were incubated with 1.8 μg of GST-tagged wild-type REV3L-N5 (N5-WT), N5-D525A, N5-G526A and N5-TD527,529AA mutants, respectively. Reactions were performed at 37°C for 30 min and resolved by 10% SDS-PAGE.

polymerase catalytic domain. Consistently, the interaction between N70 and the C-terminal catalytic domain is substantiated by reciprocal Co-IP experiments performed in HEK293 cells coexpressed with both a HA-tagged N70 and a 3xFLAG-tagged REV3L C-terminal fragment (Figure 4C, lanes 4' and 4" in lower panels). Moreover, REV7, a regulatory subunit of Pol ζ, and two accessory subunits of Pol δ, Pol D2 and Pol D3, can be coimmunoprecipitated with the 3xFLAG-tagged N70 from the nuclear exact of HCT116-3F-REV3L cells but not from HCT116 cells (Figure 4D). It has been documented that REV3, together with REV7, Pol D2 and Pol D3, forms a four-subunit Pol ζ4 complex, and Pol ζ4 complex formation is critical for the TLS activity of Pol ζ both *in vitro* and *in vivo* (9,41). Since it has been well established that the REV7-binding motifs locate within the C-terminal region of REV3L (10–14), these data unexpectedly reveal that after cleavage, the two REV3L cleavage products remain associated and participate in a functionally-active Pol ζ4 complex.

A physical link between N70 and Pol ζ4 complex implies a role of the cleaved N70 fragment for REV3L function. To test this idea, we introduced an expression cassette of the REV3L N-terminal fragment N485 (containing the extreme N-terminal 485 residues), driven by a tet-inducible promoter, into a stable HCT116 derivative that constitutively expresses a FLAG-tagged REV3L N-terminal truncation (N-tru, containing residues 526–3130, identical to the C-terminal cleavage product of REV3L) by lentiviral transduction (Figure 4E, lanes 3 and 4). Strikingly, the expression of REV3L N485 fragment markedly represses levels of the phosphorylated RPA2 at residue Threonine (Thr) 21 and H2AX at Serine (Ser) 139 (γ-H2AX) following a

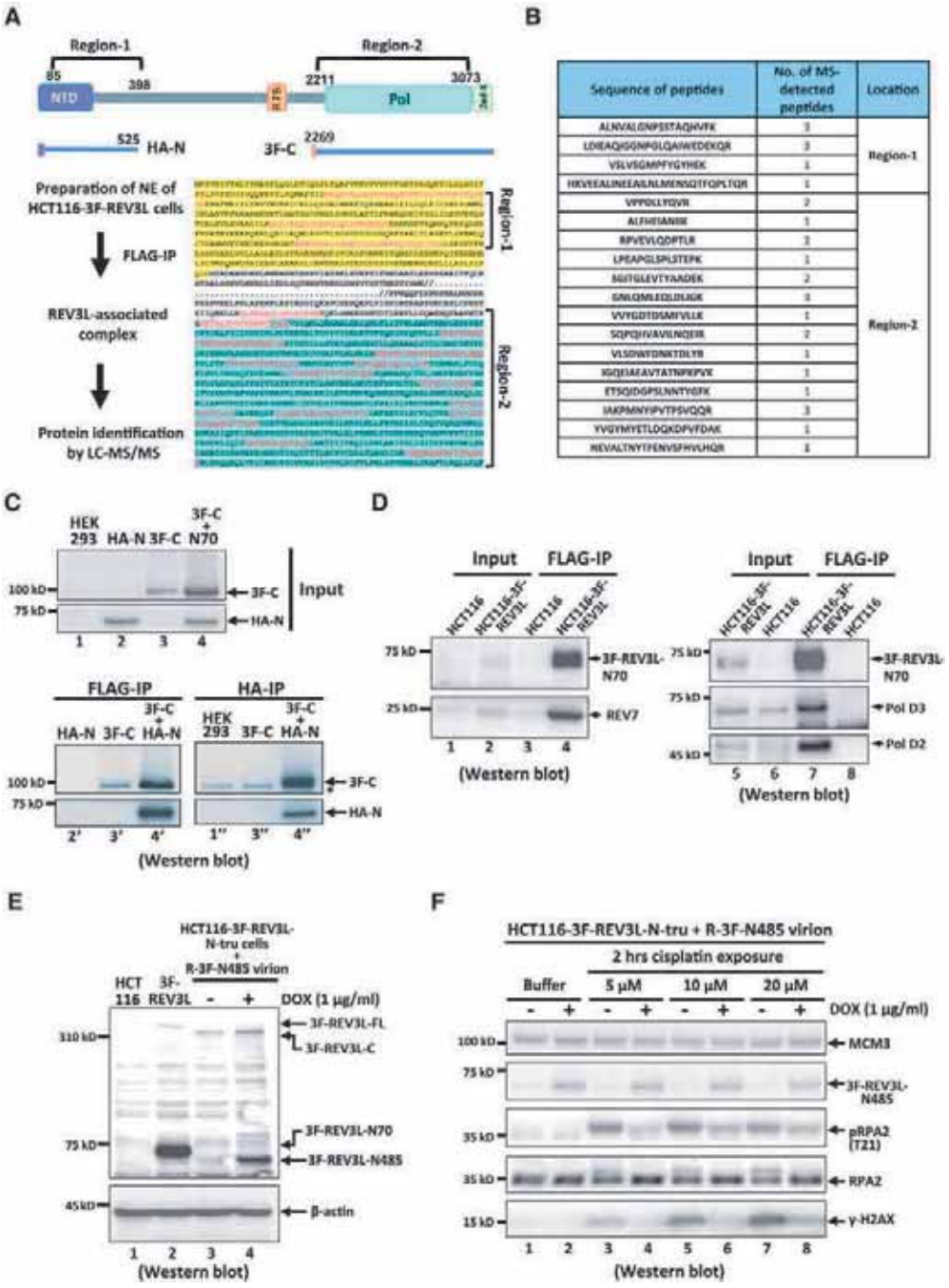

Figure 4. Both cleaved fragments of REV3L form a post-cleavage complex and synergistically function in alleviating cisplatin-induced replication stresses and genomic instability. (**A**) Top panel: A diagram showing REV3L functional domains. Lower-left panel: The strategy for purification of N70-associated proteins from the nuclear extract of HCT116-3F-REV3L cells. Lower-right panel: Sequences of tryptic peptides detected by MS are shown in red letters. The N70 sequence is highlighted in yellow, whereas the C-terminal polymerase catalytic domain of REV3L is highlighted in cyan. (**B**) A summary of the MS-detected tryptic peptides. (**C**) The C-terminal catalytic domain of human REV3L interacts with N70 in HEK293 cells. Schematic representation of 3xFLAG-tagged (3F-C) and HA-tagged REV3L (HA-N) truncations transiently expressed in HEK293 cells is shown in (A). Thirty-six hours after transfection, whole cell lysates were subjected to reciprocal Co-IP analyses using anti-FLAG and anti-HA antibodies. The levels of indicated proteins in lysates (top panel) and Co-IP samples (lower-left and lower-right panels) were monitored by immunoblotting. A non-specific band detected by anti-FLAG antibody in HA-IPed samples is indicated by an asterisk. (**D**) The N-terminal cleavage product of 3xFLAG-tagged REV3L is associated with components of Pol ζ4 complex in HCT116-3F-REV3L cells. The indicated proteins in lysates and Co-IP samples were detected by western blot. (**E**) Expression of FLAG-tagged REV3L variants was monitored by western blot. A doxycycline-inducible FLAG-tagged REV3L-N485 truncation expression cassette was stably integrated into HCT116-3F-N-tru cells by lentiviral transduction. Cells were grown in the presence or absence of 1 μg/ml doxycycline (DOX) for 24 h prior to harvest. β-actin was detected as a loading control. Lysates from HCT116 and HCT116-3F-REV3L cells were used as controls for anti-FLAG immunoblotting. (**F**) Phosphorylation of Chk1, RPA2, and H2AX was monitored by western blot at 24 h following a 2-h exposure to cisplatin at the indicated doses in HCT116-3F-REV3L-N-tru cells with (+DOX) or without (–DOX) doxycycline-induced 3F-REV3L-N485 expression.

2-h cisplatin exposure at various doses (Figure 4F, lanes 4, 6 and 8 in comparison with lanes 3, 5 and 7). In contrast, ectopic expression of REV3L N-terminal fragments only has a marginal effect on the cisplatin-induced phosphorylation of both proteins in HCT116 cells and cells with depleted REV3L (Supplementary Figure S6). The phosphorylation of RPA2 (Thr21, Ser33) is specifically modified by ATR to signal the presence of replication stress (42). Levels of γ-H2AX, a marker of double-strand DNA breaks (DSBs) (43), reflect negative impacts of cisplatin-induced replication stresses on genome integrity. These results, together with the fact that the N-terminal cleavage product is involved in a functionally-active Pol ζ4 complex, support that both cleavage products synergistically function in preventing cisplatin-induced replication stresses and genomic instability in HCT116 cells.

Full-length REV3L undergoes K48-linked poly-ubiquitination and proteasomal degradation

The above studies uncover a sequence-dependent proteolytic event involved in the post-translational processing of human REV3L. Since TASP1 is involved in the maturation of a group of nuclear transcription factors that are critical for cell growth and proliferation in mammals (33,44,45), we decided to address the role of the TASP1-mediated REV3L proteolysis in human cells by generating a derivative of HCT116-3F-REV3L cells bearing defined point mutations at both alleles of the *REV3L* gene that lead to alanine substitutions at the Q-L-D-G-T-A-D motif of REV3L. Mutations were introduced by CRISPR/Cas9n-mediated genome editing (Figure 5A). The positive colonies were first identified by restriction mapping and then verified by sequencing a 182-bp region flanking the mutated nucleotides at the *REV3L* locus (Figure 5B–D). Considering the detrimental effect of REV3L inactivation on cell growth (Supplementary Figure S2), we initially set out to establish a derivative of HCT116 cells, expressing a cleavage-deficient REV3L mutant carrying two alanine substitutions at T527 and D529. As expected, while no significant difference is found on the rates of cell growth and proliferation between the TD527, 529AA mutant cells (3F-TD-Mut) and the cells carrying the wild-type *REV3L* gene (3F-WT) (Supplementary Figure S7), two alanine substitutions result in a sharp decrease in the cleavage product N70 in the mutant cells (Figure 5E), consistent with the critical role of D529 in REV3L cleavage. Strikingly, while the nucleotide substitutions have no observable effect on the steady levels of the *REV3L* mRNA in mutant cells (Figure 5F), a sharp decrease in the cleavage product N70 does not proportionally accompany an increase in the full-length REV3L proteins in the cleavage-deficient TD527, 529AA mutant cells. As compared to the cleavage-competent wild-type cells, the total amount of FLAG-tagged REV3L proteins in mutant cells is markedly decreased (Figure 5E). This raised a possibility that the full-length REV3L may have a significantly shorter half-life than N70. However, to our surprise, a 24-h proteasome inhibitor MG132 treatment resulted in a marked increase in the abundance of the cleavage product N70, but not the full-length protein in the TD527,529AA mutant cells (Supplementary Figure S8A). Paradoxically, MG132 treatment has no observable effect on the stability of N70 in wild-type HCT116-3F-REV3L cells (Figure 6A, bottom panel).

Considering that T527A and D529A mutations impair but do not completely abolish REV3L cleavage, we reasoned that an increase in the amount of the cleavage product N70 could also result from an elevated stability of the full-length protein in the MG132-treated mutant cells. To clarify this possibility, we decided to establish a completely cleavage-inactive REV3L mutant cell line by substituting the essential cleavage residue D525 with an alanine in the endogenous *REV3L* gene in HCT116 cells. A two-step genome engineering strategy was applied to introduce defined point mutations at one of the *REV3L* alleles in the heterozygous (het) HCT116-3F-REV3L cell line, which led to two alanine substitutions at residues D525 and T527 of REV3L (Figure 5G). Successful targeting was verified by both genomic DNA PCR and sequencing a 374-bp region flanking the mutated nucleotides in the *REV3L* cDNA (Figure 5H and I). To facilitate detection of REV3L-D525A mutant protein, only the HCT116-3F-REV3L-D525A-mut cells, which bear mutations at the *REV3L* allele carrying the 3xFLAG tag coding sequences, were used in the subsequent experiments.

The aforementioned *in vivo* and *in vitro* studies have established that the D525 residue is essential for REV3L cleavage. In keeping with this notion, the amount of the cleavage product N70 was reduced to levels undetectable by western blot in REV3L-D525A mutant(het) cells (Figure 5K, line 3, Supplementary Figure S8B, lane 4). While the steady-state levels of *3F-REV3L* mRNA are comparable in both cell lines (Figure 5J, lane 3 in comparison with lane 2), the total amount of FLAG-tagged REV3L protein in D525A mutant cells is markedly reduced to only around 16% of that in parental HCT116-3F-REV3L(het) cells (Figure 5K), reminiscent of the cleavage-deficient TD527, 529AA mutant cells.

To assess the impact of REV3L cleavage on its protein stability, the half-life of both the cleavage-inactive D525A mutant and the cleavage product N70 of wild type REV3L was determined by blocking *de novo* protein synthesis with cycloheximide (CHX) for different times. As shown in Figure 6A and B, the full-length REV3L-D525A mutant is profoundly less stable than the cleavage product N70 of the wild type REV3L. More importantly, MG132 treatment markedly stabilizes the full-length REV3L-D525A protein in the mutant cells (Figure 6A, top panel), but not the cleavage product N70 in parental HCT116-3F-REV3L(het) cells (Figure 6A, bottom panel).

The above data suggest that the stability of non-cleavable REV3L-D525A mutant is negatively regulated by the ubiquitin-proteasome system. Indeed, we found that non-cleavable REV3L-D525A proteins immunopurified from the MG132-treated mutant cells under denaturing conditions (in the presence of 1 M urea), carry K48-linkage-specific poly-ubiquitin chains (Figure 6C, lane 4 in the middle and bottom panels). Compatible with the conjugation of poly-ubiquitin chains to the mutant proteins, the ubiquitinated REV3L-D525A proteins migrate significantly slower than the main band of the FLAG-tagged mutant proteins on SDS-PAGE (Figure 6C, lane 4 in the middle and bot-

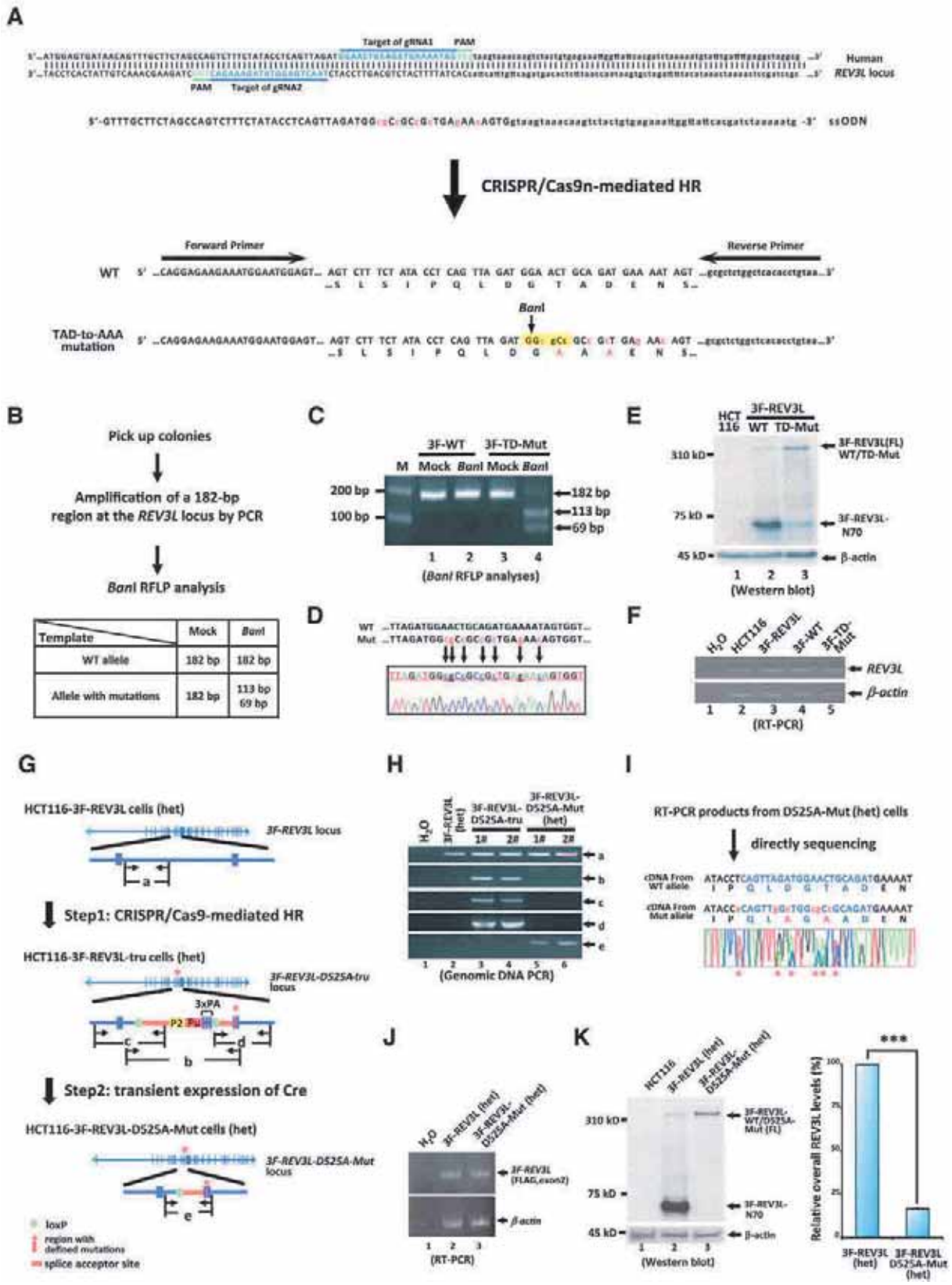

Figure 5. Alanine substitutions at the Q-L-D-G-T-A-D motif significantly decrease the abundance of REV3L in HCT116 cells. (**A**) A schematic illustration of the strategy for establishing a REV3L-TD527,529AA mutant cell line by CRISPR/Cas9n-mediated genome engineering approach. The locations of the

tom panels in comparison with the corresponding lane in the top panel).

To clarify whether the ubiquitination of REV3L-D525A mutant would be attributed to alanine substitutions, we immunopurified REV3L proteins from the extracts derived from the MG132-treated wild type HCT116-3F-REV3L cells. Of note, K48-linked poly-ubiquitin conjugates were also detected on the wild-type full-length REV3L proteins immunopurified under denaturing conditions (Figure 6D, lanes 5′ and 5″). In keeping with the modification of the non-cleaved wild type REV3L proteins with K48-linked ubiquitin chains, the full-length wild type REV3L protein in MG132-treated HCT116-3F-REV3L cells can be pulled down under harsh denaturing conditions (in the presence of 6 M guanidine hydrochloride) by an ectopically expressed His8-HA-tagged wild-type or mutant ubiquitin that bears arginine substitutions at all lysine (K) residues except K48 (K48), but not by one bearing arginine substitutions at all 7 K residues (7R) (Figure 6E, lanes 6 and 7 in comparison with lane 8). Moreover, similar to what was observed for the immunopurified REV3L, the His8-HA-ubiquitin pulled-down REV3L species show a significantly slower SDS-PAGE migration than the main band of the full-length proteins (Figure 6E, lanes 6 and 7). These data, together with the well-established notion that K48-linked poly-ubiquitin chains are targeted for proteasomal degradation (46–48), strongly support that the full-length REV3L, both wild-type and the D525A mutant, is a labile protein targeted for K48-linked poly-ubiquitination and proteasomal degradation, suggesting that TASP1-mediated proteolysis plays an indispensable role in protecting REV3L from the ubiquitin-proteasome system in human cells.

Cellular responses to UV- and cisplatin-induced DNA lesions are significantly impaired in cleavage-defective REV3L mutant cells

To further assess the biological significance of the REV3L proteolytic event identified in the above studies, we first set out to define biological consequences of a lack of REV3L in HCT116 cells. To this end, we took advantage of a *REV3L* conditional knockout HCT116 derivative, in which the transcription of both *REV3L* alleles is driven by a tetracycline (tet)-inducible promoter (Supplementary Figure S9D and S9E). Thus, expression of REV3L could be simply repressed by withdrawal of doxycycline (dox) from the medium in this line (Supplementary Figure S10A). Consistent with a well-defined TLS activity of Pol ζ in bypassing UV- and cisplatin-induced DNA damage (1,2), our data indicate that inactivation of REV3L severely impairs cellular response to UV- and cisplatin-induced DNA lesions in HCT116 cells. First, by carefully examining the accumulation of nuclear RPA foci at different time points following UV irradiation, we found that UV irradiation-induced nuclear RPA foci accumulate faster and disappear much more slowly in REV3L-depleted cells than in cells with REV3L expression, indicating that REV3L activity is critical for alleviating UV damage-induced replication stress in human cells (Supplementary Figure S10B). Second, depletion of REV3L severely impairs the relief of replication stresses resulting from cisplatin-induced DNA lesions, reflected in the appearance of persistent phosphorylation of both Chk1 at Ser317 and RPA2 at Thr21 at 6, 12 and even 24 h after a 2-h exposure to 4 μM cisplatin in REV3L-depleted cells (Supplementary Figure S10C, lanes 8–12). In contrast, only marginal levels of the phosphorylation of both proteins was detected in REV3L-competent cells at all tested time points following a cisplatin exposure (Supplementary Figure S10C, lanes 2–6). Concomitant with the accumulation of extensive replication stresses following a cisplatin exposure, inactivation of REV3L also poses negative impacts on genome integrity, reflected by a significant increase in levels of γ-H2AX in the REV3L-depleted cells after a cisplatin exposure as compared with those in the REV3L-expressed cells (Supplementary Figure S10C). In addition, depletion of REV3L also causes a ∼79% reduction in mutation frequency of the UV-irradiated pSP189 plasmids replicated in HCT116 cells (Supplementary Figure S10D). This may reflect the fact that Pol ζ replicates damaged DNA with very low fidelity as its catalytic subunit REV3L lacks a proofreading exonuclease activity (1–3), and in agreement with some previous studies indicating that REV3L is responsible for the vast majority of UV-induced mutations in both yeast and human cells (4,5,8,26).

By taking advantage of the above established biological consequences linked to REV3L inactivation in HCT116 cells, we next set out to assess whether cleavage is important for REV3L function by utilizing the cleavage-deficient REV3L-TD527,529AA-mutant (TD-mut) cells. We found that, in comparison with the cleavage-competent wild-type

←

gRNAs and ssODN are indicated. Blue bars and letters indicate the positions of the gRNA targets with green bars highlighting the PAM sequences. The substituted nucleotides in ssODN are shown in red letters. The deduced amino acid sequences from wild-type (WT) and mutated sequences are shown at the bottom, with red letters indicating nucleotide and amino acid substitutions. A *Ban*I site resulting from nucleotide substitutions is highlighted by a yellow box. (**B**) Strategy for genotyping by genomic DNA PCR and *Ban*I restriction-fragment length polymorphism (RFLP) analyses. (**C**) Results of *Ban*I RFLP analyses of representative cell lines with (3F-TD-Mut) or without (3F-WT) TD527,529AA substitutions in the *REV3L* locus. A 182-bp region surrounding the gRNA target site was PCR amplified from the genomic DNAs. PCR products were subjected to *Ban*I digestion. Sizes of fragments are indicated. (**D**) Sequences of the PCR fragment from the 3F-TD-Mut cell line as shown in (C). The substituted nucleotides are underlined. (E, F) Both cleavage and the steady levels of REV3L are markedly decreased in cells with biallelic substitutions. Cells were assayed for the indicated proteins and mRNAs by western blot (**E**) and RT-PCR (**F**), respectively. (**G**) Schematic of a two-step genome targeting strategy for establishing a heterozygous REV3L-D525A mutant cell line. Green circle: *loxP* site. Red asterisk: defined mutations. Brown box: splice acceptor site. (**H**) Genotyping by genomic DNA PCR. Locations of PCR primers are indicated in (G). (**I**) The sequencing result of the RT-PCR fragment derived from the total RNAs of a HCT116-3F-REV3L-D525A mutant cell line. The expected sequences of the RT-PCR products from the WT allele and the mutant allele, together with their encoding amino acids, are presented. The substituted nucleotides are highlighted in red. Heterozygous peaks (double peak) are indicated by red asterisks. (J–K) Cells were assayed for the indicated mRNAs and proteins by RT-PCR (**J**) and western blot (**K**), respectively. The relative abundances of 3xFLAG-tagged REV3L-D525A-Mut and N70 proteins in (K) are quantified by ImageJ and plotted as indicated in right panel of (K). Error bars represent standard deviations from three independent experiments. *P* values were determined using two-tailed Student's *t*-test. $^{***}P < 0.0001$, $t = -254.14$, df = 2.

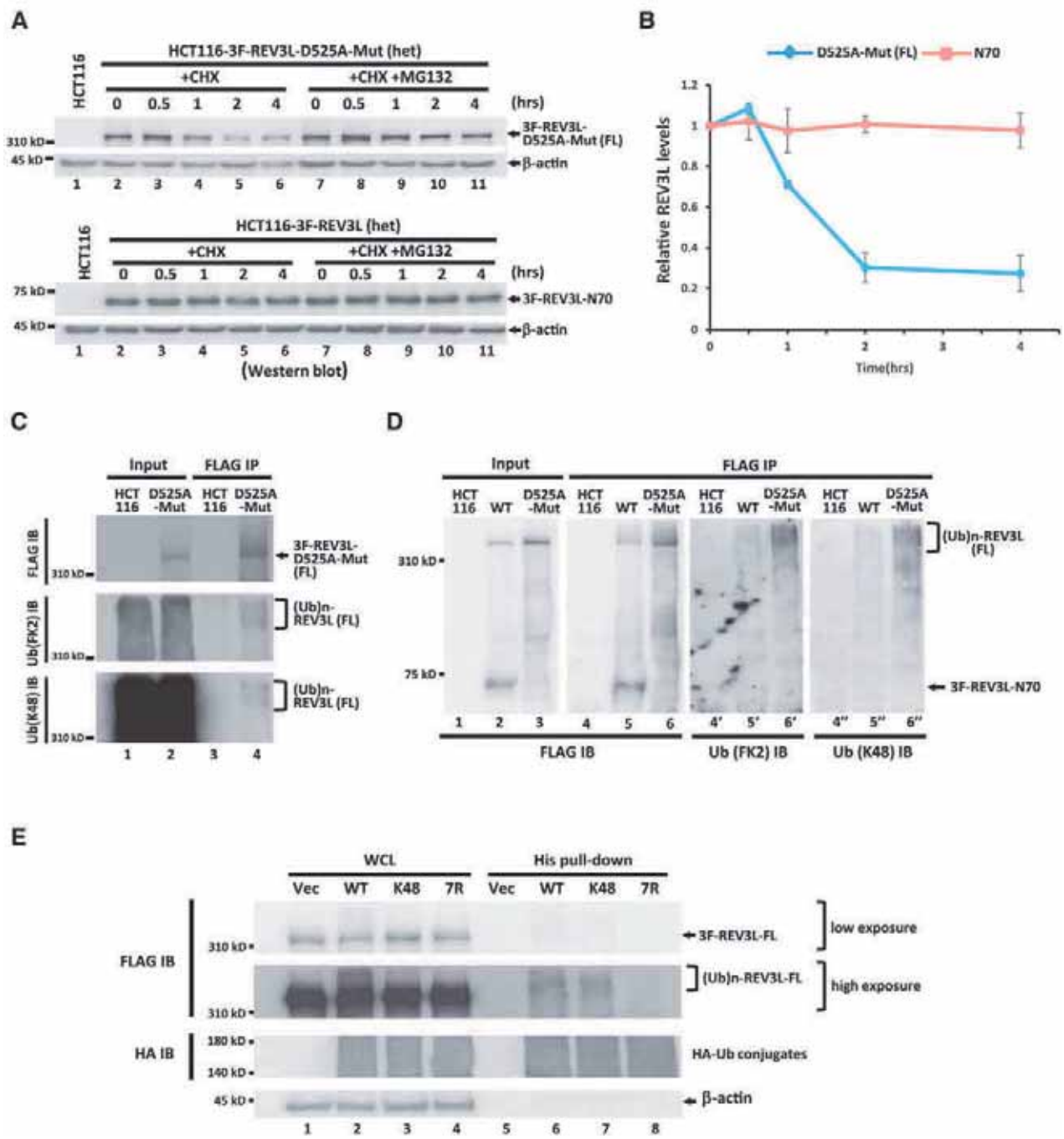

Figure 6. The full-length REV3L undergoes ubiquitination and proteasome-mediated degradation. (**A**) Full-length REV3L protein undergoes proteasome-mediated degradation. The indicated protein in HCT116-3F-REV3L-D525A-Mut (het) and HCT116-3F-REV3L (het) cells was monitored by western blot. (**B**) The relative abundances of 3xFLAG-tagged REV3L-D525A-Mut and N70 proteins in (A) (lanes 2–6) are quantified by ImageJ. Error bars represent standard deviations from three independent experiments. Diamond, 3F-REV3L-D525A mutant. Square, 3F-REV3L-N70. (**C**) REV3L-D525A mutant protein is conjugated with K48-linked poly-ubiquitin chains. The indicated proteins in Input and anti-FLAG IPs from HCT116 and HCT116-3F-REV3L-D525A-Mut cells were analyzed by immunoblotting analyses (IB). Ub(FK2) IB: detect K29-, K48-, K63-linkage specific ubiquitination. Ub(K48) IB: detect K48-linkage specific ubiquitination. (**D**) Full-length wild-type REV3L undergoes K48-linked poly-ubiquitination. The indicated protein levels in Input and anti-FLAG IPs were assessed by IB analyses as described in (C). (**E**) IB analyses of whole cell lysates (WCL) and His pull-down products derived from HCT116-3F-REV3L cells transfected with plasmids expressing His8-HA-tagged ubiquitin or ubiquitin-K48 or −7R mutant as indicated. His pull-down analyses were performed in the presence of 6 M guanidine hydrochloride.

cells, both accumulation of UV-induced RPA foci (Figure 7A and B, Supplementary Figure S11), and levels of the phosphorylated RPA2 in the mutant cells following UV irradiation and cisplatin exposures are significantly increased (Figure 7C and D), supporting that a deficiency of cleavage significantly impairs the involvement of REV3L in alleviating UV- and cisplatin-induced replication stresses. Moreover, the *SupF* mutation frequencies of the pSP189 plasmid replicated in the TD-mutant cells are significantly reduced to levels comparable to those in the aforementioned REV3L-depleted cells (Figure 7E, Supplementary Figure S10D). Together, these data suggest a significant loss of REV3L activity in the cleavage-deficient TD-mut cells.

To directly assess the biological consequence of a lack of REV3L cleavage, we set out to generate two HCT116 derivatives, R-REV3L-WT(het) and R-REV3L-CI-mut(het) cell lines (Figure 8A and B, Supplementary Figure S9). A fragment carrying a transcription termination signal, a tetracycline (tet)-inducible promoter and the sequences coding a 3xFLAG tag was integrated into one of the *REV3L* alleles in both lines, immediately upstream to the coding region of an endogenous *REV3L* gene (Supplementary Figure S9D and E). Defined point mutations, which lead to an alanine substitution at the essential cleavage residue D525 in REV3L, were simultaneously introduced into the second *REV3L* allele in the R-REV3L-CI-mut(het) cells (Supplementary Figure S9A–C), but not in the R-REV3L-WT(het) cells. Thus, the expression of the wild type FLAG-tagged REV3L could be simply repressed by withdrawal of dox from the medium in both lines (Figure 8C). This leads to an exclusive expression of non-tagged REV3L proteins, either wild-type or cleavage-inactive D525A mutant, derived from the *REV3L* gene that is under the control of an endogenous *REV3L* promoter in the relative lines.

We next took advantage of these two cell lines to assess the activity of the cleavage-inactive REV3L-D525A mutant in alleviating UV- and cisplatin-induced replication stresses. As compared to the dox-withdrawn R-REV3L-WT(het) cells, a significant delay of the clearance of UV-induced RPA foci and phosphorylation of RPA2 and Chk1 proteins was observed in the dox-withdrawn mutant cells that solely express non-cleavable REV3L-D525A mutant proteins (Figure 8D and the right panel of Figure 8E), analogous to what was observed in the cleavage-deficient TD-Mut cells. In contrast, both RPA foci and the phosphorylation of RPA2 and Chk1 were eliminated at comparable rates in wild-type and mutant cells in the presence of dox (8D and the left panel of 8E).

Also consistent with a loss of REV3L activity in cells singly expressing D525A mutant, both accumulation of replication stresses and formation of DSBs were sharply increased in the dox-withdrawn mutant cells following a 2-h 4 μM cisplatin exposure as compared to those in the dox-withdrawn wild-type cells (Figure 8F, lanes 8′–12′ in comparison with lanes 8–12). Concomitant with an elevated level of DSBs formation, we also observed sharp increases in the frequency of micronuclei formation in the dox-withdrawn mutant cells following a 12-hr exposure to 5 μM cisplatin as compared to those of cells with wild-type REV3L expression (Figure 8G). Together, these data reveal a severe loss of REV3L activity in cells solely expressing non-cleavable REV3L-D525A mutant protein.

DISCUSSION

In this study, we report a previously-unrecognized proteolytic event of human REV3L. We further demonstrate that such a post-translational cleavage event prevents ubiquitination and degradation of human REV3L, and is indispensable for the function of REV3L involved in cellular response to UV- and cisplatin-induced DNA damage. These findings uncover a new means of modulating the abundance of REV3L through site-specific proteolysis in human cells.

Human REV3L is about twice as large as its yeast ortholog (8). Strikingly, the characterized Q-L-D-G-T-A-D motif, which is critical for REV3L proteolysis, is embedded in a region that is absent in its yeast counterpart. Our finding thus reveals a functional relevance of the human-specific sequence in modulating the expression of REV3L. It is noted that the Q-L-D-G-T-A-D motif sequence in REV3L remains identical from chicken to human and the N-terminal cleavage products naturally occur in various mouse tissues, suggesting that the site-specific proteolysis of REV3L is a conserved physiological event in metazoans. Given the importance of cleavage for the modulation of REV3L activity *in vivo* as revealed in this study, understanding whether and how REV3L cleavage is coordinated into cellular responses to various genotoxic stresses will be an attractive topic for future research.

The key aspect of our model is that REV3L undergoes a site-specific proteolytic event. Failure of this event results in ubiquitination and proteasome-mediated degradation of REV3L. Due to lack of an available antibody, we are unable to directly monitor the C-terminal cleavage product of REV3L. However, given the fact that the C-terminal fragment participates in a functionally-active Pol ζ4 complex (9,41) and acts together with the N-terminal cleavage product N70 in response to cisplatin-induced DNA damage, we reason that the C-terminal cleavage product is very unlikely to be a labile protein, which warrants future in-depth study.

How might a proteolysis event protect REV3L from the ubiquitin–proteasome system? A short-lived protein targeted for the ubiquitin–proteasome system usually contains a degradation signal called a ‘degron’ (49). A degron comprises multiple determinants that have different roles in the degradation pathway. For instance, some sequences or structural elements within the degron determine the recognition of the ubiquitin–ligase complex, whereas one or multiple other residue(s) of the degron serves as an acceptor site(s) for the attachment of poly-ubiquitin chains. Hence, the TASP1-mediated cleavage may protect REV3L from the ubiquitin–proteasome system by interrupting the degron structure or by physically dissociating the conjugation site(s) of poly-ubiquitin chains from the element(s) required for ubiquitin–ligase complex recognition. Structural analysis of both full-length and cleaved REV3L variants, together with the characterization of the degradation signal and ubiquitin conjugation site(s), will provide necessary information to evaluate these possibilities in future in-depth studies.

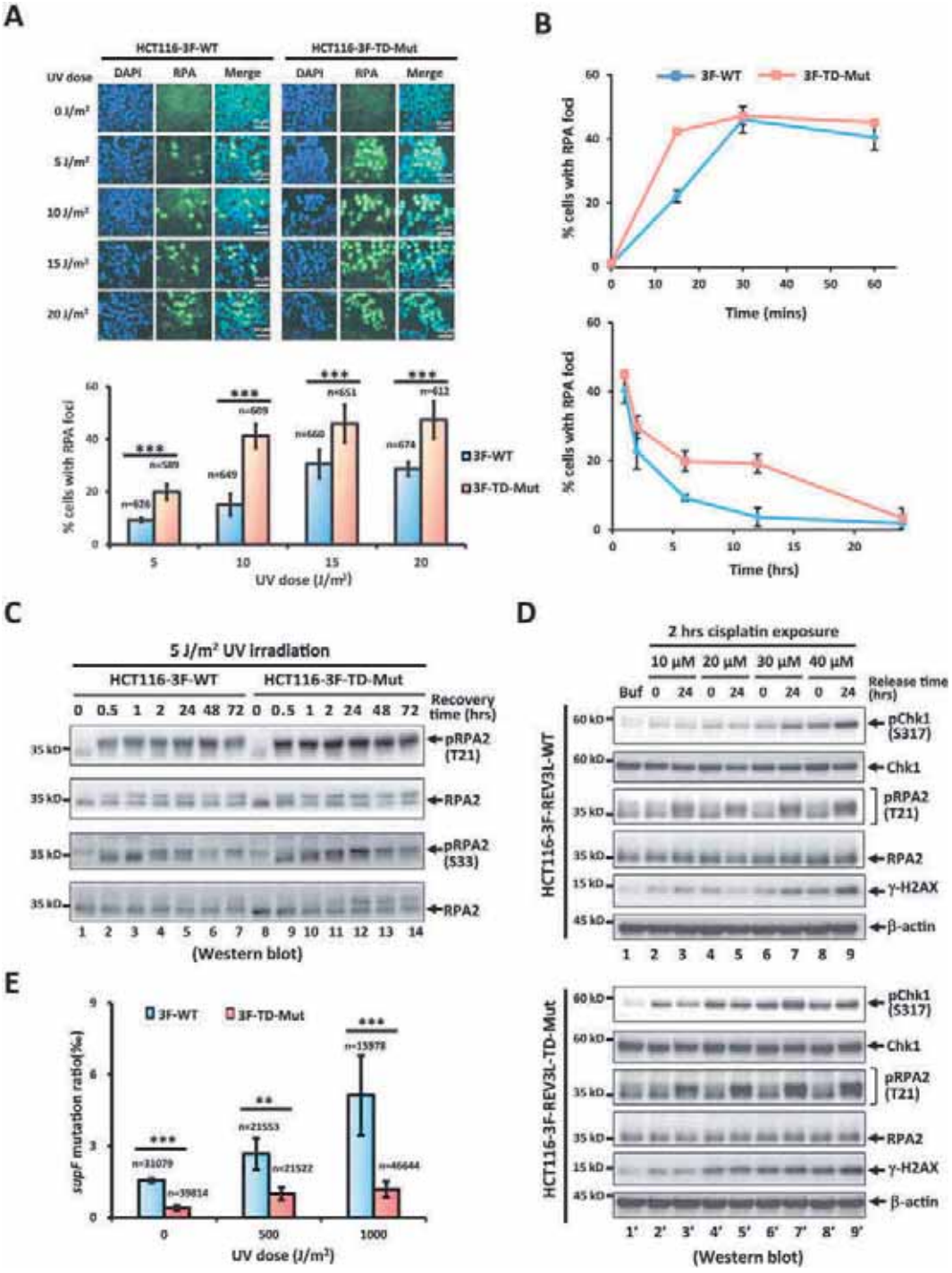

Figure 7. Cellular responses to UV- and cisplatin-induced DNA lesions are impaired in cleavage-deficient REV3L-TD527, 529AA mutant cells. (**A**) RPA focus analyses in REV3L cleavage-competent (3F-WT) and cleavage-deficient (3F-TD-Mut) HCT116 cells at 6 h after UV irradiation at the indicated doses. Top panel: Representative images. Scale bar, 40 μm. Bottom panel: Quantitative analyses of cells with positive RPA foci. The number of cells scored for each condition is indicated. (**B**) Time-course analyses of accumulation (top panel) and clearance (bottom panel) of RPA foci in 3F-WT and 3F-TD-Mut cells following 5 J/m^2 UV irradiation. For each cell line at each time point at least 100 cells were counted. Circle, 3F-WT cells. Square, 3F-TD-Mut cells. (**C**) Phosphorylation of RPA2 at T21 and S33 residues was monitored by western blot at the indicated time points following 5 J/m^2 UV irradiation in HCT116 cells expressing wild-type (3F-WT) or mutant (TD-Mut) REV3L. Expression of RPA2 was determined as loading control. (**D**) Phosphorylation of Chk1, RPA2 and H2AX was monitored by western blot 24 h post-exposure to cisplatin at the indicated doses in wild-type or TD-Mut cells. Expression of Chk1, RPA2 and β-actin was determined as loading controls. (**E**) Mutation frequencies of UV damaged *sup F* plasmid (0, 500 or 1000 J/m^2 UV-C irradiated), replicated in REV3L cleavage competent (3F-WT) and deficient (3F-TD-Mut) HCT116 cell derivatives, were determined. Replicated *supF* plasmids were isolated 48 h after transfection. The number of colonies scored for each condition is indicated. In all cases, data are presented as mean ± SD from three independent experiments. *P* values in (A) and (E) were determined using Pearson's Chi-squared test. $^{**}P < 0.001$, $^{***}P < 0.0001$.

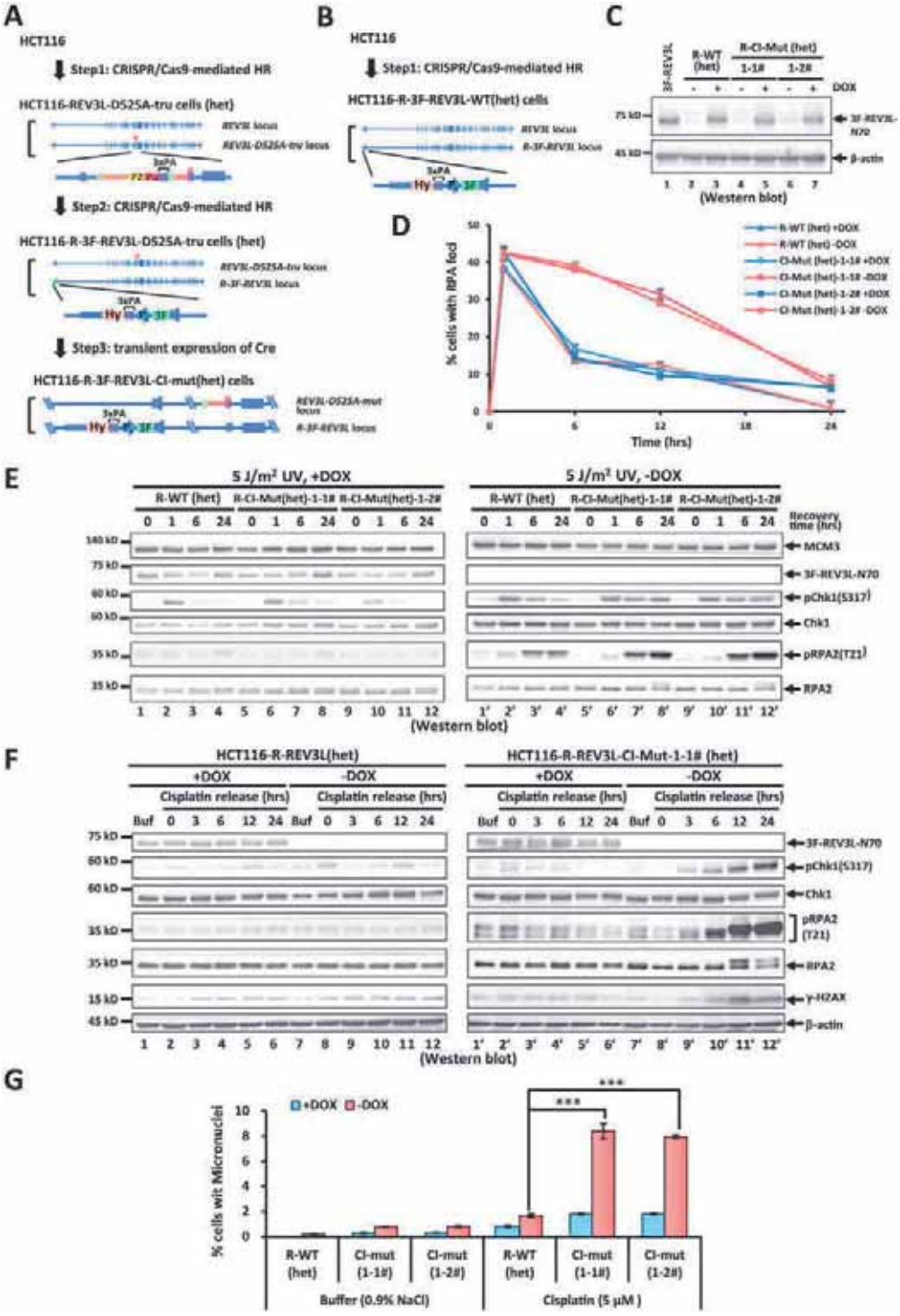

Figure 8. The activities of REV3L are markedly decreased in cleavage-inactive REV3L mutant cells. (A and B) Schematic of genome targeting strategies for establishing HCT116-R-3F-REV3L-CI-Mut(het) (**A**) and HCT116-R-3F-REV3L-WT(het) (**B**) cell lines. (**C**) Expression of 3xFLAG-tagged REV3L and β-actin was monitored by western blot in the indicated HCT116 derivatives. R-WT(het): HCT116-R-3F-REV3L-WT(het) cell. R-CI-Mut(het): HCT116-R-3F-REV3L-CI-Mut(het) cells. (**D**) Time-course analyses of accumulation of RPA foci in the indicated cells after 20 J/m^2 UV irradiation. For each cell line at each time point at least 100 cells were counted. Curves for cells with (+DOX) or without (–DOX) induction of 3xFLAG-tagged wild type REV3L are shown in brown and blue, respectively. Triangle, R-WT(het) cells. Circle, CI-Mut-1-1 cells. Square, CI-Mut-1-2 cells. (**E**) Phosphorylation of Chk1 and RPA2 was measured by western blot at various time points after 5 J/m^2 UV irradiation in the indicated cells. (**F**) Phosphorylation of Chk1, RPA2 and H2AX was monitored by western blot at various time points following a 2-h exposure to 4 μM cisplatin in the indicated cells. (**G**) Frequencies of micronuclei formation were quantified in the indicated cells following a 12-h exposure to 5 μM cisplatin. Data are presented as mean ± SD from three independent experiments. *P* values were determined using Pearson's Chi-squared test. ***$P < 0.0001$.

TASP1 has a critical role in controlling cancer cell proliferation and apoptosis (50). It has been well established that TASP1 modulates a plethora of genetic programs through cleaving some nuclear transcription factors (33,45,51). This report uncovers a transcription-independent role of TASP1 in TLS-mediated DNA damage responses. Notably, analogous to depletion of TASP1 (50), disruption of REV3L expression results in growth inhibition and enhanced apoptosis in many human cancer cell lines, including HCT116 cells (52). An extensive body of evidence has indicated that continued cell proliferation in cancer relies heavily on replication stress responses (53). Thus, the idea that loss of TASP1 interferes with REV3L-mediated TLS and thereby induces sustained replication stress and impairments of cell proliferation remains an intriguing possibility. New insights gained from this study enhance our understanding of how TASP1 functions in human cells.

SUPPLEMENTARY DATA

Supplementary Data are available at NAR Online.

ACKNOWLEDGEMENTS

We thank Dr C. Lawrence (University of Rochester Medical Center, Rochester, NY) for providing human *REV3L* cDNA. We thank Dr S. Chen at the Proteomics Facility of NIBS for his assistance in mass spectrometry analysis at the very beginning of this study. We thank Y. Bai and Y. Yan for sharing HCT116-3F-REV3L-N-tru stable cell lines. We are grateful to Dr Z. Qin and X. Niu for their assistance with the RPA focus assay, and to M. Hanna for proofreading the manuscript.

FUNDING

Ministry of Science and Technology of the People's Republic of China [2015CB910603 to X.L.]; National Natural Science Foundation of China [31470780 to X.L.]; Capacity Building for Sci-Tech Innovation-Fundamental Scientific Research Funds [010185515800, 025185305000]. Funding for open access charge: Interdisciplinary Study Foundation of Capital Normal University.
Conflict of interest statement. None declared.

REFERENCES

1. Makarova,A.V. and Burgers,P.M. (2015) Eukaryotic DNA polymerase zeta. *DNA Repair (Amst.)*, **29**, 47–55.
2. Gan,G.N., Wittschieben,J.P., Wittschieben,B.O. and Wood,R.D. (2008) DNA polymerase zeta (pol zeta) in higher eukaryotes. *Cell Res.*, **18**, 174–183.
3. Nelson,J.R., Lawrence,C.W. and Hinkle,D.C. (1996) Thymine-thymine dimer bypass by yeast DNA polymerase zeta. *Science (New York, N.Y.)*, **272**, 1646–1649.
4. Lemontt,J.F. (1972) Induction of forward mutations in mutationally defective yeast. *Mol. Gen. Genet.*, **119**, 27–42.
5. Quah,S.K., von Borstel,R.C. and Hastings,P.J. (1980) The origin of spontaneous mutation in Saccharomyces cerevisiae. *Genetics*, **96**, 819–839.
6. Zhong,X., Garg,P., Stith,C.M., Nick McElhinny,S.A., Kissling,G.E., Burgers,P.M. and Kunkel,T.A. (2006) The fidelity of DNA synthesis by yeast DNA polymerase zeta alone and with accessory proteins. *Nucleic Acids Res.*, **34**, 4731–4742.
7. Harfe,B.D. and Jinks-Robertson,S. (2000) DNA polymerase zeta introduces multiple mutations when bypassing spontaneous DNA damage in Saccharomyces cerevisiae. *Mol. Cell*, **6**, 1491–1499.
8. Gibbs,P.E., McGregor,W.G., Maher,V.M., Nisson,P. and Lawrence,C.W. (1998) A human homolog of the Saccharomyces cerevisiae REV3 gene, which encodes the catalytic subunit of DNA polymerase zeta. *Proc. Natl. Acad. Sci. U.S.A.*, **95**, 6876–6880.
9. Lee,Y.S., Gregory,M.T. and Yang,W. (2014) Human Pol zeta purified with accessory subunits is active in translesion DNA synthesis and complements Pol eta in cisplatin bypass. *Proc. Natl. Acad. Sci. U.S.A.*, **111**, 2954–2959.
10. Tomida,J., Takata,K., Lange,S.S., Schibler,A.C., Yousefzadeh,M.J., Bhetawal,S., Dent,S.Y. and Wood,R.D. (2015) REV7 is essential for DNA damage tolerance via two REV3L binding sites in mammalian DNA polymerase zeta. *Nucleic Acids Res.*, **43**, 1000–1011.
11. Murakumo,Y., Roth,T., Ishii,H., Rasio,D., Numata,S., Croce,C.M. and Fishel,R. (2000) A human REV7 homolog that interacts with the polymerase zeta catalytic subunit hREV3 and the spindle assembly checkpoint protein hMAD2. *J. Biol. Chem.*, **275**, 4391–4397.
12. Murakumo,Y., Ogura,Y., Ishii,H., Numata,S., Ichihara,M., Croce,C.M., Fishel,R. and Takahashi,M. (2001) Interactions in the error-prone postreplication repair proteins hREV1, hREV3, and hREV7. *J. Biol. Chem.*, **276**, 35644–35651.
13. Hara,K., Hashimoto,H., Murakumo,Y., Kobayashi,S., Kogame,T., Unzai,S., Akashi,S., Takeda,S., Shimizu,T. and Sato,M. (2010) Crystal structure of human REV7 in complex with a human REV3 fragment and structural implication of the interaction between DNA polymerase zeta and REV1. *J. Biol. Chem.*, **285**, 12299–12307.
14. Hanafusa,T., Habu,T., Tomida,J., Ohashi,E., Murakumo,Y. and Ohmori,H. (2010) Overlapping in short motif sequences for binding to human REV7 and MAD2 proteins. *Genes Cells*, **15**, 281–296.
15. Morrison,A., Christensen,R.B., Alley,J., Beck,A.K., Bernstine,E.G., Lemontt,J.F. and Lawrence,C.W. (1989) REV3, a Saccharomyces cerevisiae gene whose function is required for induced mutagenesis, is predicted to encode a nonessential DNA polymerase. *J. Bacteriol.*, **171**, 5659–5667.
16. Schenten,D., Kracker,S., Esposito,G., Franco,S., Klein,U., Murphy,M., Alt,F.W. and Rajewsky,K. (2009) Pol zeta ablation in B cells impairs the germinal center reaction, class switch recombination, DNA break repair, and genome stability. *J. Exp. Med.*, **206**, 477–490.
17. Bemark,M., Khamlichi,A.A., Davies,S.L. and Neuberger,M.S. (2000) Disruption of mouse polymerase zeta (Rev3) leads to embryonic lethality and impairs blastocyst development in vitro. *Curr. Biol.*, **10**, 1213–1216.
18. Esposito,G., Godindagger,I., Klein,U., Yaspo,M.L., Cumano,A. and Rajewsky,K. (2000) Disruption of the Rev3l-encoded catalytic subunit of polymerase zeta in mice results in early embryonic lethality. *Curr. Biol.*, **10**, 1221–1224.
19. Wittschieben,J., Shivji,M.K., Lalani,E., Jacobs,M.A., Marini,F., Gearhart,P.J., Rosewell,I., Stamp,G. and Wood,R.D. (2000) Disruption of the developmentally regulated Rev3l gene causes embryonic lethality. *Curr. Biol.*, **10**, 1217–1220.
20. Lange,S.S., Wittschieben,J.P. and Wood,R.D. (2012) DNA polymerase zeta is required for proliferation of normal mammalian cells. *Nucleic Acids Res.*, **40**, 4473–4482.
21. Van Sloun,P.P., Varlet,I., Sonneveld,E., Boei,J.J., Romeijn,R.J., Eeken,J.C. and De Wind,N. (2002) Involvement of mouse Rev3 in tolerance of endogenous and exogenous DNA damage. *Mol. Cell Biol.*, **22**, 2159–2169.
22. Kajiwara,K., J,O.W., Sakurai,T., Yamashita,S., Tanaka,M., Sato,M., Tagawa,M., Sugaya,E., Nakamura,K., Nakao,K. *et al.* (2001) Sez4 gene encoding an elongation subunit of DNA polymerase zeta is required for normal embryogenesis. *Genes Cells*, **6**, 99–106.
23. Lange,S.S., Bedford,E., Reh,S., Wittschieben,J.P., Carbajal,S., Kusewitt,D.F., DiGiovanni,J. and Wood,R.D. (2013) Dual role for mammalian DNA polymerase zeta in maintaining genome stability and proliferative responses. *Proc. Natl. Acad. Sci. U.S.A.*, **110**, E687–E696.
24. Bhat,A., Andersen,P.L., Qin,Z. and Xiao,W. (2013) Rev3, the catalytic subunit of Polzeta, is required for maintaining fragile site stability in human cells. *Nucleic Acids Res.*, **41**, 2328–2339.
25. Lazzaro,F., Novarina,D., Amara,F., Watt,D.L., Stone,J.E., Costanzo,V., Burgers,P.M., Kunkel,T.A., Plevani,P. and Muzi-Falconi,M. (2012) RNase H and postreplication repair protect

cells from ribonucleotides incorporated in DNA. *Mol. Cell*, **45**, 99–110.
26. Li,Z., Zhang,H., McManus,T.P., McCormick,J.J., Lawrence,C.W. and Maher,V.M. (2002) hREV3 is essential for error-prone translesion synthesis past UV or benzo[a]pyrene diol epoxide-induced DNA lesions in human fibroblasts. *Mutat. Res.*, **510**, 71–80.
27. Lin,Y.C., Owen,N., Minko,I.G., Lange,S.S., Li,L., Stone,M.P., Wood,R.D., McCullough,A.K. and Lloyd,R.S. (2016) DNA polymerase zeta limits chromosomal damage and promotes cell survival following aflatoxin exposure. *Proc. Natl. Acad. Sci. U.S.A.*, **113**, 13774–13779.
28. Shachar,S., Ziv,O., Avkin,S., Adar,S., Wittschieben,J., Reissner,T., Chaney,S., Friedberg,E.C., Wang,Z., Carell,T. *et al.* (2009) Two-polymerase mechanisms dictate error-free and error-prone translesion DNA synthesis in mammals. *EMBO J.*, **28**, 383–393.
29. Wu,F., Lin,X., Okuda,T. and Howell,S.B. (2004) DNA polymerase zeta regulates cisplatin cytotoxicity, mutagenicity, and the rate of development of cisplatin resistance. *Cancer Res.*, **64**, 8029–8035.
30. Suzuki,T., Gruz,P., Honma,M., Adachi,N. and Nohmi,T. (2016) The role of DNA polymerase zeta in translesion synthesis across bulky DNA adducts and cross-links in human cells. *Mutat. Res.*, **791–792**, 35–41.
31. Cong,L., Ran,F.A., Cox,D., Lin,S., Barretto,R., Habib,N., Hsu,P.D., Wu,X., Jiang,W., Marraffini,L.A. *et al.* (2013) Multiplex genome engineering using CRISPR/Cas systems. *Science (New York, N.Y.)*, **339**, 819–823.
32. Li,X. and Manley,J.L. (2005) Inactivation of the SR protein splicing factor ASF/SF2 results in genomic instability. *Cell*, **122**, 365–378.
33. Hsieh,J.J., Cheng,E.H. and Korsmeyer,S.J. (2003) Taspase1: a threonine aspartase required for cleavage of MLL and proper HOX gene expression. *Cell*, **115**, 293–303.
34. Qin,Z., Lu,M., Xu,X., Hanna,M., Shiomi,N. and Xiao,W. (2013) DNA-damage tolerance mediated by PCNA*Ub fusions in human cells is dependent on Rev1 but not Poleta. *Nucleic Acids Res.*, **41**, 7356–7369.
35. Manley,J.L., Fire,A., Cano,A., Sharp,P.A. and Gefter,M.L. (1980) DNA-dependent transcription of adenovirus genes in a soluble whole-cell extract. *Proc. Natl. Acad. Sci. U.S.A.*, **77**, 3855–3859.
36. Parris,C.N. and Seidman,M.M. (1992) A signature element distinguishes sibling and independent mutations in a shuttle vector plasmid. *Gene*, **117**, 1–5.
37. Richard,D.J., Bolderson,E. and Khanna,K.K. (2009) Multiple human single-stranded DNA binding proteins function in genome maintenance: structural, biochemical and functional analysis. *Crit. Rev. Biochem. Mol. Biol.*, **44**, 98–116.
38. Hsieh,J.J., Ernst,P., Erdjument-Bromage,H., Tempst,P. and Korsmeyer,S.J. (2003) Proteolytic cleavage of MLL generates a complex of N- and C-terminal fragments that confers protein stability and subnuclear localization. *Mol. Cell Biol.*, **23**, 186–194.
39. Bier,C., Knauer,S.K., Klapthor,A., Schweitzer,A., Rekik,A., Kramer,O.H., Marschalek,R. and Stauber,R.H. (2011) Cell-based analysis of structure-function activity of threonine aspartase 1. *J. Biol. Chem.*, **286**, 3007–3017.
40. Chen,D.Y., Lee,Y., Van Tine,B.A., Searleman,A.C., Westergard,T.D., Liu,H., Tu,H.C., Takeda,S., Dong,Y., Piwnica-Worms,D.R. *et al.* (2012) A pharmacologic inhibitor of the protease Taspase1 effectively inhibits breast and brain tumor growth. *Cancer Res.*, **72**, 736–746.
41. Makarova,A.V., Stodola,J.L. and Burgers,P.M. (2012) A four-subunit DNA polymerase zeta complex containing Pol delta accessory subunits is essential for PCNA-mediated mutagenesis. *Nucleic Acids Res.*, **40**, 11618–11626.
42. Vassin,V.M., Anantha,R.W., Sokolova,E., Kanner,S. and Borowiec,J.A. (2009) Human RPA phosphorylation by ATR stimulates DNA synthesis and prevents ssDNA accumulation during DNA-replication stress. *J. Cell Sci.*, **122**, 4070–4080.
43. Rogakou,E.P., Pilch,D.R., Orr,A.H., Ivanova,V.S. and Bonner,W.M. (1998) DNA double-stranded breaks induce histone H2AX phosphorylation on serine 139. *J. Biol. Chem.*, **273**, 5858–5868.
44. Oyama,T., Sasagawa,S., Takeda,S., Hess,R.A., Lieberman,P.M., Cheng,E.H. and Hsieh,J.J. (2013) Cleavage of TFIIA by Taspase1 activates TRF2-specified mammalian male germ cell programs. *Dev. Cell*, **27**, 188–200.
45. Zhou,H., Spicuglia,S., Hsieh,J.J., Mitsiou,D.J., Hoiby,T., Veenstra,G.J., Korsmeyer,S.J. and Stunnenberg,H.G. (2006) Uncleaved TFIIA is a substrate for taspase 1 and active in transcription. *Mol. Cell Biol.*, **26**, 2728–2735.
46. Chau,V., Tobias,J.W., Bachmair,A., Marriott,D., Ecker,D.J., Gonda,D.K. and Varshavsky,A. (1989) A multiubiquitin chain is confined to specific lysine in a targeted short-lived protein. *Science (New York, N.Y.)*, **243**, 1576–1583.
47. Komander,D. and Rape,M. (2012) The ubiquitin code. *Annu. Rev. Biochem.*, **81**, 203–229.
48. Finley,D. (2009) Recognition and processing of ubiquitin-protein conjugates by the proteasome. *Annu. Rev. Biochem.*, **78**, 477–513.
49. Ravid,T. and Hochstrasser,M. (2008) Diversity of degradation signals in the ubiquitin-proteasome system. *Nat. Rev. Mol. Cell Biol.*, **9**, 679–690.
50. Chen,D.Y., Liu,H., Takeda,S., Tu,H.C., Sasagawa,S., Van Tine,B.A., Lu,D., Cheng,E.H. and Hsieh,J.J. (2010) Taspase1 functions as a non-oncogene addiction protease that coordinates cancer cell proliferation and apoptosis. *Cancer Res.*, **70**, 5358–5367.
51. Takeda,S., Chen,D.Y., Westergard,T.D., Fisher,J.K., Rubens,J.A., Sasagawa,S., Kan,J.T., Korsmeyer,S.J., Cheng,E.H. and Hsieh,J.J. (2006) Proteolysis of MLL family proteins is essential for taspase1-orchestrated cell cycle progression. *Genes Dev.*, **20**, 2397–2409.
52. Knobel,P.A., Kotov,I.N., Felley-Bosco,E., Stahel,R.A. and Marti,T.M. (2011) Inhibition of REV3 expression induces persistent DNA damage and growth arrest in cancer cells. *Neoplasia*, **13**, 961–970.
53. Hanahan,D. and Weinberg,R.A. (2011) Hallmarks of cancer: the next generation. *Cell*, **144**, 646–674.